Martin Smolnig, BSc

A new lipotoxicity pathway in yeast

MASTER'S THESIS

to achieve the university degree of

Master of Science

Master's degree programme: Molecular Microbiology

submitted to

Graz University of Technology

Supervisor

Prof., Frank Madeo

Institute for molecular Biosciences
Karl-Franzens University of Graz

Dr. Patrick Rockenfeller
Kent Fungal Group, University of Kent (UK)

Graz, May 2016

AFFIDAVIT

I declare that I have authored this thesis independently, that I have not used other than the declared sources/resources, and that I have explicitly indicated all material which has been quoted either literally or by content from the sources used. The text document uploaded to TUGRAZonline is identical to the present master‘s thesis dissertation.

Date

Signature

Acknowledgements

Works like this are made possible by the combined effort of many people to hurriedly overcome bureaucratic hurdles and issues of expertise resulting in another interested member of the scientific society.

Now I would like to express my thanks to the people, who did that for me. Firstly, I express my gratitude to Prof. Frank Madeo, who got me interested in cell death research. Working under supervision of Dr. Patrick Rockenfeller has been an invaluable experience in terms of disillusionment and practical skills.

Companies often praise themselves by promoting their working atmosphere. The year I spent as part of the Madeo Group introduced me to excellent climate both at work as well as after hours. I would like to thank Joakim Franz and Ines Fößl for invaluable teamwork in the lab, and Andreas Zimmermann for his patient statistics explanations. In times of doubt the Bergler, Pertschy and Büttner groups lent a necessary, helping hand just as well.

Expecting a timely end to their child's studies is the right of all parents. Mine had to remain patient a little longer, thanks for doing so. Support in my family has been good at all times, especially my sisters and uncle had a part in that.

On a different note I would like to extend my thanks to my good friends, who have taught me to rise, when I was down and pointed out the obvious when I was too confused to see it. Thanks Rebekka for the rare interdisciplinary discussions, I honestly appreciate those. Thanks Thomas for the repeated reminder what science is all about.

Timendi causa est nescire.

Lucius Annaeus Seneca

Abstract

Lipotoxicity, the detrimental effects of lipids on organisms, is caused by lipid overflow in non-adipose tissue. The corresponding health issues have become more pressing in the past decades with increasing occurrence of lipid metabolism associated diseases. In this study lipotoxicity was examined on a cellular level in *Saccharomyces cerevisiae* with focus on the toxic effects of diacylglycerol (DAG). The administration of a DAG species, which is not physiological in yeast, 1,2-dioctanoyl-*sn*-gycerol (DOG), has been shown to cause necrotic cell death previously. In the here-presented master thesis I investigate the molecular mechanisms involved in the DOG metabolism and resulting cellular demise. Applying sensing molecules for DAG and different phospholipid (PL) species enabled microscopic tracking of DAG/DOG movement to observe dynamic changes in the wild type with or without DOG treatment and selected genetic knockout strains. To identify deletion strains, which show interesting effects upon DOG-treatment, clonogenic survival assays (CSA) were performed. Genes of different well-known pathways were examined during the process of DOG fate elucidation. Involvement of some pathways could be confirmed, while others only activate due to overlapping parts. DOG moves via different organelles during uptake and metabolism, which can be used to influence the resulting phenotype.

To corroborate these findings additional studies in yeast as well as in higher organisms are necessary.

Kurzzusammenfassung

Lipotoxizität, der schädliche Effekt von Lipiden auf einen Organismus, wird verursacht durch Lipidüberschuss in nichtadipösem Gewebe. Die daraus resultierenden Gesundheitsprobleme nahmen in den letzten Jahrzenten mit erhöhtem Aufkommen lipidassoziierter Erkrankungen zu. In dieser Studie wurde Lipotoxizität auf zellulärer Ebene in *Saccharomyces cerevisiae* mit Fokus auf Diacylglycerin (DAG) untersucht. Bereits gezeigt wurde, dass die Verabreichung der in Hefe nicht physiologischen DAG-Form 1,2-Dioktanoyl-sn-Glycerin (DOG) zu nekrotischem Zelltod führt. In der hier präsentierten Masterarbeit untersuche ich die molekularen Mechanismen des DOG Metabolismus und des daraus resultierenden Zelltods. Die Anwendung von Sensormolekülen für DAG und verschiedene Phospholipide (PL) ermöglichte die mikroskopische Verfolgung der DAG/DOG Route und folgender Veränderungen in Wildtypzellen und ausgewählten Knockoutstämmen. Zur Identifizierung von Deletionsstämmen, die interessante Effekte durch DOG Zugabe zeigten, wurden klonogene Überlebensplattierungen (CSA) durchgeführt. Gene verschiedener bekannter Signalpfade wurden während der Erläuterung des DOG Schicksals untersucht. Die Beteiligung mancher Pfade konnte bestätigt werden, während andere nur durch Überlappung aktiviert werden. DOG bewegt sich während Aufnahme und Metabolismus über verschiedene Organellen, die genutzt werden können um den resultierenden Phänotyp zu beeinflussen.

Um diese Erkenntnisse zu untermauern sind weitere Studien in Hefe und höheren Organismen notwendig.

Glossary

Abbreveation	Term
AcN	acetonitrile
AIF	apoptosis inducing factor
ALP	alkaline phosphatase
CFU	colony forming units
CPY	carboxypeptidase Y
CSA	clonogenic survival assay
DAG	diacylglycerol
DIC	differential interference contrast
DMSO	dimethyl sulfoxide
DOG	1,2-dioctanoyl-sn-glycerol
EE	early endosome
ER	endoplasmic reticulum
ESCRT	endosomal sorting complex required for transport
FA	fatty acid
FFA	free fatty acid
GFP	green fluorescent protein
ILV	intraluminal vesicles
IP	inositol phosphate
LD	lipid droplet
LE	late endosome
LPA	lyso-phosphatidic acid
MVB	multi-vesicular body
PA	phosphatidic acid
PARP-1	poly (ADP-ribose) polymerase 1
PC	phosphatidylcholine
PCD	programmed cell death
PE	phosphatidylethanolamine
PH	pleckstrin homology
PI	phosphatidylinositol
PI3,5P$_2$	phosphatidylinositol-3,5-biphosphate
PI3K	phosphatidylinositol-3-kinase
PI3P	phosphatidylinositol-3-phosphate
PI4,5P$_2$	phosphatidylinositol-4,5-biphosphate
PI4P	phosphatidylinositol-4-phosphate
PIP	phosphatidylinositol phosphate
PL	phospholipids
PLCδ	phospholipase C δ1
PM	plasma membrane
PS	phosphatidylserine

PTPC	permeability transition pore complex
ROS	reactive oxygen species
RT	room temperature
SMD	selective minimal media dextrose
SNARE	Soluble NSF Attachment Protein REceptor
TAG	triacylglycerol
VM	vacuolar membrane
VPS	vacuolar protein sorting
YPD	yeast peptone dextrose full medium

TABLE OF CONTENTS

1. Introduction 1
1.1. Yeast as a model organism 1
1.2. Lipotoxicity 2
1.2.1. Lipid metabolism in yeast 3
1.3. Cell death 6
1.3.1. Necrosis 7
1.3.2. Necrosis in yeast 8
1.4. The Rim101 pathway 9
1.5. Cargo internalization and trafficking 10
1.5.1. Endocytosis 10
1.5.2. Endosomal trafficking 11
1.5.3. SNARE-mediated vacuolar fusion 12
1.6. Vacuolar morphology - class A-F compartments 13
1.7. Aims of the project 13
2. Materials 14
2.1. Strains and Plasmids 14
2.2. Growth media 15
2.3. Buffers 15
2.4. Supplemental reagents 16
2.5. Instruments 17
3. Methods 18
3.1. Yeast Cultivation and Storage 18
3.2. Plasmid Transformation 18
3.3. Clonogenic Survival Assay 19
3.4. Lipid stress induction 19
3.5. Microscopy 20
3.5.1. Sensing molecules 20
3.5.2. Microscopy and digital enhancement 20
3.5.3. Cell cycle synchronisation 21
3.6. Statistical analysis 21
4. Results 22

4.1. Prevention of DOG induced cell death 22
4.1.1. Knockouts of *vps34Δ* and *snf7Δ* prevent cell death 22
4.1.2. Knockouts of SNARE-proteins prevent cell death 23
4.1.3. Knockout of *ypt32Δ* prevents cell death 23
4.2. Microscopic localisation studies 24
4.2.1. The dynamic DAG distribution upon DOG administration 24
4.2.2. DAG moves from mother to daughter cell in large amounts via vesicles originating from the vacuole 25
4.2.3. PI4,5P_2 localisation shows little difference upon DOG addition 28
4.2.4. DOG induced changes in PS localisation in wild type cells and *rim13Δ* differs in the time course. 29
4.2.5. DOG induced changes of PS localisation in vps-gene knockouts of the same class differ. 33
5. Discussion 35
5.1. DOG induced cellular demise requires the endosomal pathway 35
5.2. Impairment of vacuolar SNARE proteins prevents DOG induced cell death 35
5.3. The two yeast paralogues of Rab-GTPases of the recycling endosome affect cell death differently 36
5.4. DOG application impairs cellular DAG recycling and may repress further membrane associated processes 37
5.5. DAG distribution during cell cycle 38
5.6. PI4,5P_2 localisation upon DOG addition indicates hastened cellular demise possibly caused by ER transport blockage 39
5.7. PS localisation reveals minor, possibly ER-related differences between wild type and death preventive RIM13 knockout 40
5.8. PS localisation in vps-gene knockouts does not coincide with CSA results 41
5.9. Conclusion 42
5.10. Further experiments 43
6. Supplemental Data 45
7. References 48

1. Introduction

1.1. Yeast as a model organism

Model organisms simplify processes and by far their examinations compared to higher organisms such as mammals. Complex pathways are often hard to discover and are more comprehensive when examining simple organisms. For eukaryotic research the heterogeneous group of yeast fungi, specifically baker's yeast *Saccharomyces cerevisiae* and fission yeast *Schizosaccharomyces pombe*, have become the preferred model organisms. Both are susceptible to genomic alteration allowing for specific editing of genes of interest. While unicellular organisms do not allow for investigation of multicellular structures and organs, there are a number of conserved signalling pathways that in a similar manner lead to the same result, leavening the research process. [1]

The genome of the ascomycete *S. cerevisiae* has been completely sequenced in 1996 offering a well-researched and understood base of operations for research of cell-death and cell division cycle among others. Functional research revealed resemblance of basic mechanisms to mammalian cells, leading to the discovery of yeast orthologues to human genes.

Cell death, in its various types, can be examined by clonogenic survival assays, measurement of reactive oxygen species (ROS) and staining with fluorescent dyes, metabolically testing for either living or dead cells [2]. Further, the above mentioned high susceptibility of genomic alteration enables target-specific integration and deletion of transformed DNA, thus creating genomic backgrounds suitable for the question at hand [3]. The foremost cellular mechanism in these transformation experiments is the homologous recombination, a process much more reliable in yeast than in prokaryotes [4]. Additionally, it is possible to study non-yeast proteins in yeast by heterologous expression [5]. The expression of human genes in yeast has been used for examination of conserved pathways and disease related mutations such as Huntington's or Alzheimer's disease [6]. The expression of bovine proteins has been used as a biomarker for ubiquitous membrane particles [8].

The discovery of yeast orthologues of mammalian proteins that partake in programmed cell death proves *S. cerevisiae* as a valid model organism not just for this study [7].

1.2. Lipotoxicity

Fatty acids (FA) are a major building block for all cells. Essential to sustain life they are fundamental components of biological membranes and partake in many diverse signalling pathways. Metabolic demands of lipids and thus of FA vary greatly with the cells condition and environment. A storage form for FA is the logical requirement, realized in the form of triacylglycerols (TAG) formed by a glycerol molecule and three FA[9].

Lipid overflow in non-adipose tissue is the cause of the pathological consequence known as lipotoxicity. Lipotoxicity may even end in lipid-induced cell death or lipoapoptosis [10].

Paracelsus (1439-1541), considered the father of toxicology, is often quoted

> "Sola dosis facit venenum."
> The dose makes the poison. [11]

Nowadays lipid-associated pathologic conditions are widely spread in the modern society. Obesity, diabetes, cardiovascular diseases and adipose liver, to mention a few, are no longer abstract thoughts in the general public. Our society's omnipresent health problem due to vastly increased caloric intake, lipogenic food ranking high among it, coupled with poor physical exercise leads to a well developed interest in lipid metabolism research. Free fatty acids (FFA) have previously been identified as a likely responsible source for lipotoxicity along with ceramides, cholesterol and diacylglycerol (DAG) [12], the latter of which we focused on. FFA can be differentiated into two subspecies: saturated and unsaturated FFA. Oleic acid and linoleic acid, both unsaturated FFA, have been shown to trigger necrosis in mitochondrion-dependent manner [13]. Palmitic acid, a saturated FFA, has been shown to trigger apoptosis [14]. However in accordance to the above mentioned

Paracelsus-quote there is a limit to the cells ability of lipid uptake. Generally obesity correlates with FFA serum levels caused by overly high and chronic energy intake [15]. This surplus ends up in the accumulation of lipids and metabolic intermediates in non-adipose tissue, such as blood vessels, heart, liver, kidney and pancreas amongst others. The result is cell death in both apoptotic as well as necrotic form due to cellular dysfunctions. This pathologic condition is known as lipotoxicity [16].

The examination of lipid-induced cell death has been proven to be quite complex and thus requires the use of model organisms such as yeast. [5]

1.2.1. Lipid metabolism in yeast

Yeast cells require lipids for membrane structure of the plasma membrane (PM) and organelles like the nucleus, endoplasmic reticulum (ER), mitochondria, vacuole, peroxisomes and lipid droplets (LD), signalling pathways and cellular energy supply. Considering the ubiquitous need of lipids a highly regulated metabolism is in order. Balancing lipid storage and lipid utilisation is a complex process, only partly uncovered. Aforementioned TAG formation to store lipids includes the formation of DAG as a key intermediate (Figure 1).

DAG can serve as an FA donor to create monoacylglycerol and an FFA or an acceptor to create TAG. Alternatively DAG can be used to create phospholipids (PL) or be created from PL including phosphatidylcholine (PC), phosphatidylethanolamine, phosphatidylinositol (PI) or phosphatidic acid (PA) [17]. DAG can be created via four steps from either the glycolysis product dihydroxyacetone-3-phosphate (DHAP) or glycerol as a backbone. Both routes include lyso-phosphatidic acid (LPA) and phosphatidic acid (PA) as precursors to DAG. PA differs from DAG only by addition of a phosphate at the 3-position of the glycerol backbone. It can thus be seen as an activated form of DAG. [17]

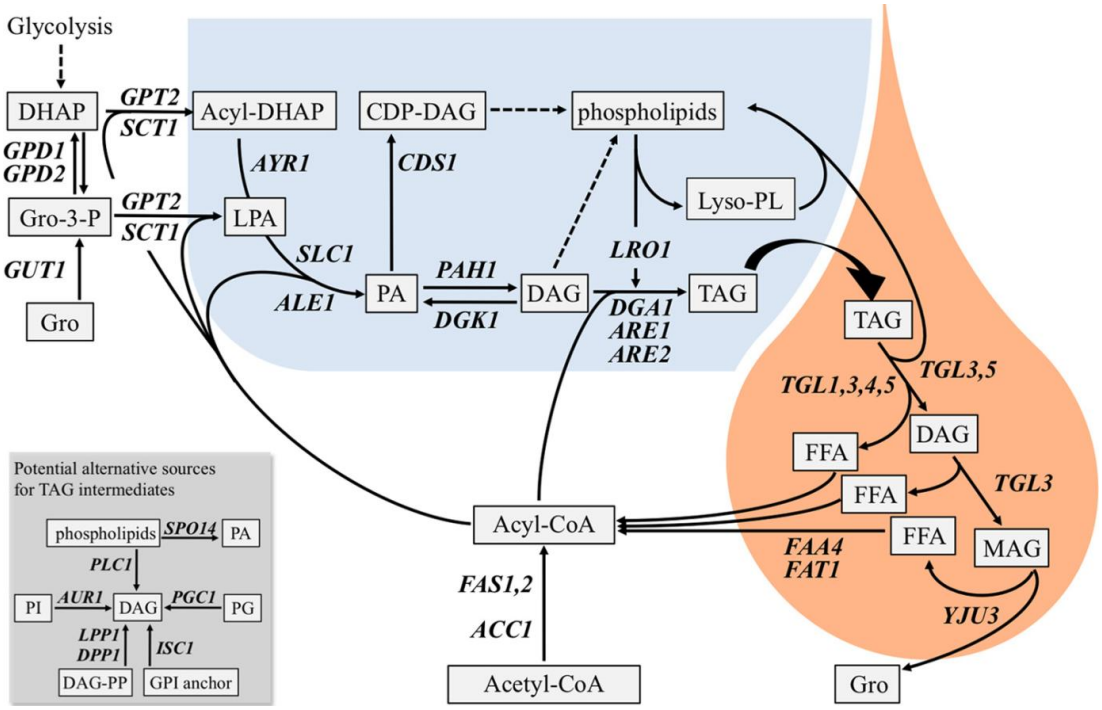

Figure 1: Enzymes involved in TAG homeostasis. (Image source: Kohlwein 2010 JBoC [17]) Blue area represents ER, red area represents LD, grey box represents alternative pathway for TAG intermediates. Gene names are italicized. Intermediates are in light grey boxes. Dashed arrows indicate multiple enzymatic steps.

While TAGs offer a valid storage form of FA, many of the cellular lipid components and signalling molecules consist of or are synthesised from PL. PA may serve as a source for phosphatidylserine (PS), which in turn serves as a source for phosphatidylethanolamine (PE) and phosphatidylcholine (PC). PS synthesis via PA uses DAG as an intermediate [18]. Deficiency in PS biosynthesis leads to formation of PE and PC via the alternative "Kennedy"-pathway. The Kennedy pathway, first described in 1956, covers PE and PC biosynthesis from ethanolamine and choline respectively [19]. Both syntheses involve three steps. PE is synthesised from ethanolamine via the ethanolamine kinase EKI1 generating phosphorylethanolamine, the PE cytidyltransferase ECT1 producing CDP-ethanolamine and the ethanolaminephosphotransferase EPT1 forming PE. PC is created from choline via CKI1 yielding phosphorylcholine, PCT1 yielding CDP-choline and CPT1 creating PC. The last steps of both formations incorporate DAG, while removing CMP. [19]

In *S. cerevisiae* PS foremost locates to the PM. Physiologically it is distributed to the inner leaflet. PS externalisation is a marker for apoptosis [20]. Bud formation and mating causes PS accumulations at the PM. Upon formation PS is delivered to the

PM via secretory vesicles. Endocytic vesicles rarely carry PS, showing its retention to the PM [21].

The phosphorylated products of PI, collectively referred to as phosphoinositides or phosphatidylinositol phosphates (PIPs), are membrane-bound lipids that function as structural components of membranes, as well as regulators of many cellular processes in eukaryotes, including vesicle-mediated membrane trafficking, cell wall integrity, and actin cytoskeleton organization. [22, 23] PIPs are also precursors of the water-soluble inositol phosphates (IPs), an important class of intracellular signalling molecules. [24, 25, 26]

The inositol ring of membrane PL and IPs are readily phosphorylated and dephosphorylated at a number of positions making them well suited as key regulators. PI can be phosphorylated at one or a combination of positions (3', 4', or 5') on the inositol head group, generating a set of unique stereoisomers that have specific biological functions. These stereoisomers have been shown to be restricted to certain membranes [22]. Phosphatidylinositol 4-phosphate (PI4P) is the major PIP species of the Golgi apparatus, where it plays a role in vesicular trafficking of secretory proteins from the Golgi to the plasma membrane [27]. Phosphatidylinositol 4,5-bisphosphate (PI4,5P_2) is the major species found at the plasma membrane and is involved in the regulation of actin cytoskeleton organization, as well as cell wall integrity, and heat shock response pathways [27]. Phosphatidylinositol 3-phosphate (PI3P) is found predominantly at endosomal membranes and in multi-vesicular bodies (MVB), where it plays a role in endosomal and vacuolar membrane trafficking [28]. Phosphatidylinositol 3,5-bisphosphate (PI3,5P_2) is found on vacuolar membranes where it plays an important role in the MVB sorting pathway [29]. PI3,5P_2 might serve as precursor to phosphatidylinositol-5-phosphate (PI5P) by 3'-phosphatases. PI5P might also be synthesised from PI directly [30]. Its role is yet to be determined, although there is evidence suggesting PI5P partakes in cell signalling and cell trafficking in mammalian blood cells. [31]. Phosphatidylinositol-3,4-bisphosphate (PI3,4P_2) might exist in very low levels in yeast evading detection so far [32]. In mammalian cells PI3,4P2 has been shown to act as a second messenger for the Akt/PKB pathway [33].

Phosphorylation and dephosphorylation of the inositol head groups of PIPs at specific membrane locations signals the recruitment of certain proteins essential for vesicular transport. [23] PIPs recruit proteins that contain PIP-specific binding domains, such as the well-studied pleckstrin homology (PH) domain that recognizes the phosphorylation pattern of specific PIP inositol head groups. [22]

In this study we used sensing molecules for PS, PI4,5P_2 as well as DAG (section 2.1 Table 2). For lipid stress induction we used the DAG 1,2-dioctanoyl-*sn*-glycerol (DOG) (Figure 2) [34]. The membrane-permeable DOG, does not appear physiologically in yeast, but is subject to lipid metabolism all the same [35, 36]. Yeast´s expected reaction to DOG administration is its acylation [37] and subsequent storage as TAG [38]. These unphysiological TAGs then further give rise to PL harbouring octanoyl residues. This may lead to instability of the PM any other PL membrane due to the change in the dynamic properties of the unphysiological PL species [39]. As an alternative route TAG degradation may also lead to release of octanoic acid as an FFA [40].

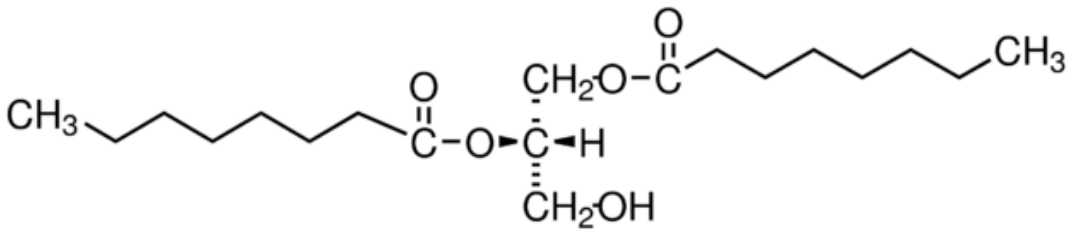

Figure 2: 1,2-Dioctanoyl-sn-glycerol (DOG) (sigmaaldrich.com) was used for induction of lipid stress.

1.3. Cell death

Cell death is not always a sudden or accidental phenomenon. It is often a highly regulated process that comes in different morphological forms. Today we differentiate between three different types of programmed cell death (PCD) that have a common denominator, which is the irreversible loss of cell membrane integrity [42]. Apoptosis (type I cell death) has long been used as a synonym for PCD. Nowadays it is considered that the controlled suicide program also extends to autophagic cell death (type II) and certain types of necrosis (type III) [43]. Morphological

characteristics of apoptosis are loss of asymmetric distribution of PM phospholipids especially PS externalisation, chromatin condensation, DNA fragmentation, PM blebbing and the formation of apoptotic bodies within the cell [42]. Autophagic cell death is void of chromatin condensation or apoptotic bodies, but shows autophagic vacuolisation [42]. The morphological features of necrosis are cell volume increase, organelle swelling, PM swelling and random DNA degradation [44].

1.3.1. Necrosis

Initially necrosis was only being regarded as an accidental, unregulated cell death process involving PM disruption caused by physical or chemical forces [45]. The disruption causes the release of factors that do not appear in apoptotic or autophagic cell death [45, 46]. Amongst those are inflammation- or immune response-inducing factors such as interleukins or cytokines. The initial understanding of necrosis was extended when infections by microorganisms showed necrotic cell death just as well as a blunt force trauma [5]. Interest spiked by these findings showed that necrosis is prominent in ischemia and neurodegenerative diseases [13].

The initiation of programmed necrosis, also referred to as 'necroptosis', by death receptors (such as tumour necrosis factor receptor 1) requires the kinase activity of receptor-interacting protein 1 (RIP1) and RIP3, and its execution involves the active disintegration of mitochondrial and lysosomal membranes as well as the PM. RIP1 and RIP3 are serine/threonine kinases [47]. Further there are several enzymes involved in necrosis, among these are cyclophilin D, poly (ADP-ribose) polymerase 1 (PARP-1) and apoptosis inducing factor (AIF) [48]. AIF is released by the mitochondria upon stimulation by PARP-1, a DNA repair protein. This shows that both apoptosis as well as necrosis are linked to mitochondrial dysfunction. Mitochondrial dysfunction leads to ROS accumulation and Ca^{2+} release that further disintegrate the mitochondrial membranes by inducing the opening of the permeability transition pore complex (PTPC). Opening of the PTPC is mediated by members of the pro-apoptotic Bcl-2 protein family. [48]

1.3.2. Necrosis in yeast

Induction of necrosis in yeast has been achieved by addition of H_2O_2, acetic acid [45] and copper, while manganese induces preferably apoptotic cell death [50]. Importantly, the amount of applied substances does significantly matter, allowing for apoptosis at lower concentration, but switching to necrosis upon higher concentrations [49]. Additionally, it turns out that the metal ions copper and manganese induce apoptosis via different pathways [50].

DOG induced cell death appears to be non-apoptotic since the gene deletion of YCA1 (yeast caspase 1) and AIF1 (apoptosis inducing factor 1), two major yeast apoptosis regulators, did not affect cellular demise [51, 52]. AnnexinV/Propidium iodide co-staining allows for discrimination between necrotic and apoptotic cell death. Apoptotic cells show AnnexinV-positive signal, primary necrosis is marked by propidium iodide positive cells. Double positive cells are in secondary stage of necrosis [4, 45]. The high-mobility-group protein Nhp6A amongst others has been shown to suppress necrosis during nutrient stress [53]. DOG treated yeast wild-type cells predominantly show propidium iodide positive signal. Nhp6A-EGFP translocated from the nucleus to the cytosol. Both these phenotypes suggest necrotic cell death. (unpublished data)

On the cellular level necrosis appears to be tightly linked to lysosomes and peroxisomes [45]. The yeast equivalent to the lysosome is the vacuole. As a degradation apparatus the vacuole is a key player in the cellular homeostasis [46]. Dysfunctional cellular homeostasis and the resulting pH-change may lead to cell death by release of pro-necrotic vacuolar proteins e.g. Pep4 and non-vacuolar proteases such as cathepsins or calpains [48, 49]. The *S. cerevisiae* proteome does include a calpain-like protease (Cpl1/Rim13 - Rim13 will be used further on), which features a full catalytic triad consisting of cysteine^{128}, histidine^{271} and asparagine^{296}. Rim13 is a yeast orthologue of mammalian calpain [54]. It is activated as part of a pH-dependant signalling cascade, the Rim101 pathway. Interestingly, *rim13Δ* did stop the cellular demise upon DOG treatment (unpublished data).

1.4. The Rim101 pathway

Rim101 is a Cys2His2-zinc finger transcriptional repressor activated upon external alkalization and mediating alkaline response genes. It is also involved in cell wall assembly and sporulation. [55]

Rim101 is proteolytically activated by the calpain-like protease Rim13. The signalling cascade that leads to the Rim101 cleavage starts at the PM and includes endosomal and vacuolar proteins [56, 57]. The pathway itself can be pictured as a two module system comprised of the sensing module and the proteolytic module. The sensing module includes Dfg16, Rim21, Rim9 and Rim8 [58, 59]. The external pH is sensed by Rim21, while Dfg16 and Rim9 regulate the delivery of Rim21 to the PM and stabilize it. [60, 61]

Initially, signal transduction process was believed to occur at the late endosome, but more recent studies revealed that recruitment of the proteolytic triad to the PM seems to initiate Rim101 activation. This is in accordance with the *Aspergillus nidulans* alkaline response pathway. [62, 63, 64, 65]

The downstream proteins Rim8, Rim20 and Rim13 accumulate at the PM but not at the late endosome upon external alkalization. Snf7, a subunit of the endosomal sorting complex required for transport 3 (ESCRT-III), partly translocates from the endosome to the PM upon alkaline pH. The ESCRT-III complex consists of four proteins forming two subunits of two proteins each. Snf7 and Vps20 form a subunit; Vps24 and Did4 form the other. Vps4, an AAA-ATPase, disassembles the complex. AAA-ATPases are a protein family associated with diverse cellular activities acting in a energy-dependant manner to remodel macromolecules. Disassembly requires the interaction of Vps4 and Vps24. Knockout of either *VPS4* or *VPS24* permanently actives the complex by preventing its disassembly. On the other hand *SNF7* deletion leads to inactivation. [57]

The prevention of DOG-induced cell death in *rim13Δ* raises the question, if the Rim101 pathway itself is mediating the DOG-induced phenotype or if it just partakes in the cellular response.

1.5. Cargo internalization and trafficking

1.5.1. Endocytosis

Addition of DOG to the growth media causes the cells to die displaying a necrotic phenotype. Unpublished data showed that DOG enters the cells and octanoyl-side chains are found in phospholipids as well as triglycerids. But how can DOG enter the cell?

Endocytosis is the process of the cell to collect extracellular material or surface proteins associated to the PM such as receptors or sensing molecules. It is an actin-dependant key mechanism in regulation of PM composition [66]. Endocytosis packs the engulfed material (cargo) into vesicles that are separated from the PM and enabled to travel to their destination. Clathrin mediated endocytosis can be structured into three phases of altogether nine steps: the immobile phase (site selection, recruiting of coat and adapter proteins, initial membrane curvature, membrane invagination), the mobile phase (slow inward mobile phase, scission, fast mobile phase) and the patch dissolution phase (recycling of coat proteins and fusion with the endosome). [66]

In the immobile phase the cargo molecules are recognized by endocytic adaptors via sorting signals. The adaptors proceed to couple the cargo to the coat. Either short peptide motifs or covalently attached ubiquitin molecules serve as sorting signals. The transition from the immobile to the mobile phase is termed maturation. In the mobile phase the cargo is internalized and the vesicle is separated via scission from the PM. Thus it is enabled to move in the cytoplasm. The actin network is assembled in this phase and interacts with a part of the coat proteins. In the patch dissolution phase the coat proteins are recycled leaving the vesicle with a lipid double layer membrane that can fuse with the endosome. The coat recycling is dominated by protein kinases that disrupt coat protein interactions by phosphorylation, thus prompting disassembly. Next to recycling the uncoating is necessary to allow for vesicle fusion with the endosome. [66]

1.5.2. Endosomal trafficking

The endosome takes up the cargo after fusion with the endocytic vesicle. The fusion mechanism is not yet totally understood [67]. However, there appears to be involvement of Vps34, the only yeast phosphoinositide-3-kinase (PI3K) synthesizing PI3P. PI3K is required for protein sorting between Golgi and vacuole. Mutation of this kinase results in dysfunctional endocytosis [67]. Additionally, by application of wortmannin, a fungal PI3K inhibitor, inhibition of endosomal fusion has been reported. This defect has been complemented by overexpression of the Rab-family GTPase on the early endosome (EE). [68]

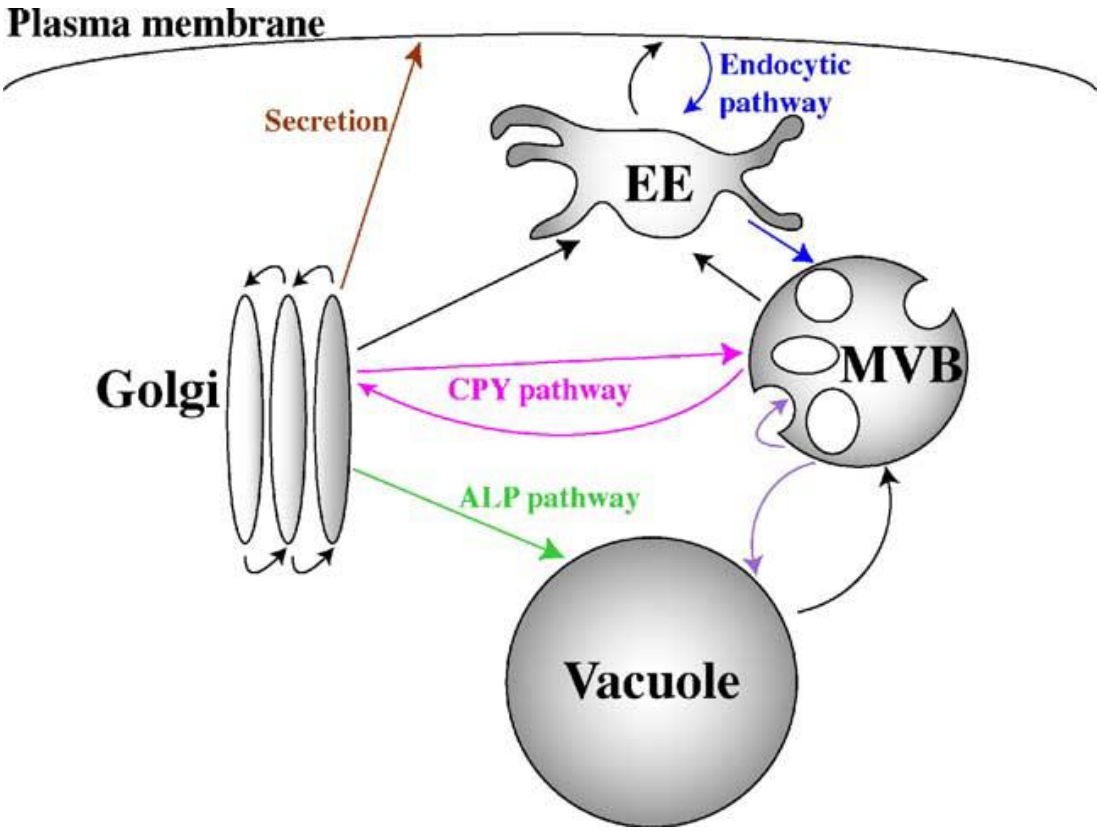

Figure 3: Protein trafficking between endosome, Golgi and vacuole in yeast. (Image source Bowers Stevens 2005 BBA **[69]**)

The further trafficking of the cargo via the endosome leads to maturation of the endosome from the EE to the late endosome (LE), which is also known as the MVB. The endosomal stages are differentiated by their surface proteins and morphological appearance. The EE exhibits among others the Rab-GTPase Ypt52, an orthologue to mammalian Rab5, while the MVB contains Ypt7, which is the Rab7 orthologue. The

LE was termed MVB due to the appearance of intraluminal vesicles (ILV). There are a number of pathways connecting the Golgi with the EE, the MVB and the vacuole, endocytosis and secretion. The best-known pathways among these are the carboxypeptidase Y (CPY) and alkaline phosphatase (ALP) pathways, which are both named after their cargos [69]. While CPY transfers cargo between Golgi and MVB, the ALP pathway bypasses the endosomal route and delivers directly from Golgi to the vacuole (Figure 3). Here we focus on the endocytic pathway. [69]

1.5.3. SNARE-mediated vacuolar fusion

After maturation into the MVB, it delivers its cargo into the vacuole by fusion with the vacuole-membrane (VM). This fusion is mediated by SNARE proteins (Soluble *N*-ethylmaleimide-sensitive factor Attachment Protein REceptor). SNARE proteins are a large group of proteins mediating vesicle fusions all over the cell. Every SNARE consists of four proteins forming the fusion complex and one GTPase to disassemble the complex. These four proteins are classified as Q_A, Q_B, Q_C and R-SNARE. The glutamine-contributing Q-SNAREs are located on one membrane, while the arginine-contributing R-SNARE is located on the other. The fusion also requires the membrane tethering factors, Sec1/Munc18 proteins and small Rab-GTPases. In case of the MVB fusion with the vacuole the SNARE in question consists of Ykt6 (R), Vam3 (Q_A), Vti1 (Q_B) and Vam7 (Q_C). The Rab-GTPase Ypt7 mediates the fusion event. The tethering factors are provided by the HOPS (homotypic fusion and protein sorting) complex. Ykt6 and Vti1 take part in other SNAREs as well and turn out to be essential proteins for cellular viability. [69, 70]

Regarding the exocytosis pathway, the recycling endosome (RE) has to be mentioned. Internalized molecules can be subjected to the PM either straight from the EE or via the RE. The RE is typically located deeper inside the cell and thus allows for interaction with the vacuole and Golgi. Aside from surface proteins and location, RE differ in terms of pH, which turns out to be slightly higher than in the EE. The key function of RE is to connect the endocytic pathway to the exocytic pathway [71]. The Rab-GTPase Ypt31 serves as a biomarker for the recycling endosome along its paralogue Ypt32. The genetic double knockout of *ypt31Δ* and *ypt32Δ* is inviable. Ypt3lp/Ypt32p-depleted cells are unable to secrete invertase, they

accumulate Golgi and ER forms of vacuolar hydrolases and they build up numerous stacks of membrane-enclosed compartments which resemble stacked Golgi cisternae found in mammalian and higher plant cells. [72]

1.6. Vacuolar morphology - class A-F compartments

Genes, coding for proteins involved in vacuolar protein sorting (VPS), have been classified into six classes (A-F) due to the vacuolar morphology caused by their mutants. Many of those over 70 genes have been identified multiple times and classified into two or more functional groups e.g. VPS34 alias is END12 [73].

Vacuolar morphology of class A resembles the wild type featuring up to ten spherical vacuoles in one area of the cytoplasm. In dividing cells the vacuole extends from mother to daughter along the cell axis. Class B compartments are fragmented vacuoles, generally small and in high amount of over twenty. Cells of class C show no identifiable vacuole. Class D compartments are single, large vacuoles that do not extend into the daughter cell. Class E cells present vacuoles larger than the wild type featuring a large prevacuolar compartment (class E compartment) that could originate from the MVB. Finally class F mutants show one large vacuole surrounded by fragmented vacuolar structures.

Mutants used in this study include *vam7Δ* (class B), *vps34Δ* (class D), *vps24Δ* and *snf7Δ* (class E). [69]

1.7. Aims of the project

This project tries to unravel the molecular mechanisms leading to cellular demise due to DOG addition in the growth media, including

- Plasma membrane rearrangement
- Pathways and organelles involved in DOG metabolism
- Involvement of the Rim101 pathway
- DOG movement inside the cell

2. Materials

2.1. Strains and Plasmids

Strains used in this study are listed in Table 1; plasmids are listed in Table 2.

Table 1: Strains used in this study

Yeast strain	Genotype	Reference
bar1Δ	*MATa his3Δ1 leu2Δ0 met15Δ0 ura3Δ0 bar1Δ::kanMX*	Euroscarf (Frankfurt, Germany)
BY4741 (WT)	MATa *his3Δ1 leu2Δ0 met15Δ0 ura3Δ0*	Euroscarf (Frankfurt, Germany)
rim13Δ	*MATa his3Δ1 leu2Δ0 met15Δ0 ura3Δ0 rim13Δ0::kanMX*	Euroscarf (Frankfurt, Germany)
snf7Δ	*MATa his3Δ1 leu2Δ0 met15Δ0 ura3Δ0 snf7Δ::kanMX*	Euroscarf (Frankfurt, Germany)
vam3Δ	*MATa his3Δ1 leu2Δ0 met15Δ0 ura3Δ0 vam3Δ::kanMX*	Euroscarf (Frankfurt, Germany)
vam7Δ	*MATa his3Δ1 leu2Δ0 met15Δ0 ura3Δ0 vam7Δ::kanMX*	Euroscarf (Frankfurt, Germany)
vps24Δ	*MATa his3Δ1 leu2Δ0 met15Δ0 ura3Δ0 vps24Δ::kanMX*	Euroscarf (Frankfurt, Germany)
vps34Δ	*MATa his3Δ1 leu2Δ0 met15Δ0 ura3Δ0 vps34Δ::kanMX*	Euroscarf (Frankfurt, Germany)
ypt31Δ	*MATa his3Δ1 leu2Δ0 met15Δ0 ura3Δ0 ypt31Δ::kanMX*	Euroscarf (Frankfurt, Germany)
ypt32Δ	*MATa his3Δ1 leu2Δ0 met15Δ0 ura3Δ0 ypt32Δ::kanMX*	Euroscarf (Frankfurt, Germany)
ypt7Δ	*MATa his3Δ1 leu2Δ0 met15Δ0 ura3Δ0 ypt7Δ::kanMX*	Euroscarf (Frankfurt, Germany)

Table 2: Plasmids used in this study

Plasmid	Description	Reference
PS-Sensor	p416-GFP-Lact-C2. Bovine Lactadherin-C2 domain	Tony Yeung [8]
DAG-Sensor	pCC4-GFP-PKD1-C1. Mural protein kinase D-C1 domain	Patrick Rockenfeller (unpublished data)
PI4,5P_2-Sensor	pRS426-GFP-2xPH(PLCδ). Rat phospholipase C-δ pleckstrin homology domain	Scott Emr [67]

2.2. Growth media

Contents of growth media are listed in Table 3.

Table 3: Growth media and contents. Substances in parentheses were used situational.

Media	Contents
YPD (full medium)	1% yeast extract 2% bacto peptone 4% D-glucose (2% agarose)
SMD (minimal media) + Amino acids	0.17% yeast nitrogen base 0.5% ammonium sulphate 2% D-glucose (80 mg/mL histidine) 200 mg/mL leucine (300 mg/mL uracil) 30 mg/mL adenine 30 mg/ml of all other amino acids (2% agarose)
LB-media	0.5 % NaCl 0.5 % yeast extract 1 % bactotryptone (0.1 mg/ml ampicillin)

2.3. Buffers

Solutions for cell density measurement at the CASY cell counter (Schärfe systems) are listed in Table 4.

Table 4: CASYton for CASY cell counter

Solution	Contents
CASYTON	0.9 mM NaCL 0.1 mM EDTA

Yeast transformation buffers and carrier DNA are listed in Table 5. TE, LiAc and PEG solutions were used for the transformation event, while SORB-Buffer was used for storage of recipient cells at -80°C.

Table 5: Yeast tranformation buffers.

Solution	Contents
10x TE	100 mM Tris/HCl, pH 7.5 10 mM EDTA/NaOH, pH 8.0
10x LiAc	1 M Lithium Acetate in H2O
50 % PEG 4000	50% Polyethylene glycol 4000 in H2O
Carrier DNA	Salmon sperm DNA (10 mg/mL)
SORB-Buffer	100 mM LiAc 1x TE 1 M sorbitol/acetic acid pH 8

2.4. Supplemental reagents

Cell cycle synchronisation was performed using reagents in Table 6.

Table 6: Reagents for cell cycle synchronisation.

Reagent	Company
α-Factor	Zymo Research
Nagase	Sigma

Lipid stress was induced by addition of DOG diluted in acetonitrile (AcN) (Table 7).

Table 7: Reagents for lipid stress induction and corresponding control.

Reagent	Company
Acetonitrile (AcN)	LOBA Feinchemie
1,2-dioctanoyl-*sn*-glycerol (DOG)	Cayman chemicals

Plasmid isolation was performed using the Thermo Scientific GeneJET Miniprep Kit abiding by the manufacturer's procedure.

DNA amount was measured using NanoDrop™ Spectrophotometer.

Propidium iodide (Unilab technologies, 100 µg/ml) was used to stain necrotic cells in microscopy experiments.

2.5. Instruments

Instruments used in this study and corresponding manufacturer are listed in Table 8.

Table 8: Instruments used in this study.

Instrument	Manufacturer
Analytical Balance	Sartorius
Autoclave	Systec
CASY Cell Counter TT	Schärfe System
Centrifuge	Eppendorf Centrifuge 5403
Centrifuge (table top)	Eppendorf Centrifuge 5418
Colony Counter	Lemna Tec
Fluorescence microscope	Zeiss Axioskop
NanoDrop Spectrophotometer	Thermo Scientific
pH meter	Metrohm
Photometer	Genesys
Thermomixer	Eppendorf Thermostat plus
Vortexer	Scientific Industries
Water distillation	GFL Dest 2208

3. Methods

3.1. Yeast Cultivation and Storage

All growth media were prepared as shown in Table 3 and were autoclaved for 25 min at 121°C and 210 kPa. Amino acids were separately autoclaved (10x-stocks), stored at -20°C, and were added after the media reached a temperature of about 50°C. For solid media like agar plates 2% agar was added. Selective minimal media (SMD) lack certain amino acids like Leu or nucleotides like Ura. Liquid media was stored at room temperature (RT), while solid media was kept at 4°C. Yeast strains were mixed with 25% glycerol and kept at -80°C for long time storage. For experiments they were streaked out on an appropriate agar plate (YPD or SMD) and were incubated for at least two days at 28°C. Liquid cultures like overnight cultures were incubated at aerobic conditions at 28°C under constant shaking at 145 rpm. *E. coli* strains were grown on LB-medium containing ampicillin and were cultivated at 37°C.

3.2. Plasmid Transformation

Transformation was performed by lithium-acetate method. Buffers were autoclaved and stored at room temperature. Carrier DNA was stored at -20°C. Before use it was denatured for 10 min at 95°C and kept on ice until use. Cells were grown over night, OD_{600} was measured and set to 0.2 in 30 ml for further culturing until OD_{600} = 0.6 was reached (4-5h). Cells were then harvested (3,500 rpm, 3 min, room temperature), washed with 10 ml H_2O and 5 ml SORB-buffer. SORB was removed by aspiration. Carrier DNA was beforehand heated for 10 min at 95°C and kept on ice until use. Cell pellet was resuspended in 360 µl SORB-buffer + 40 µl Carrier DNA. The cells were aliquoted into appropriate portions and stored at -80 °C until use. (Storage can be forgone, if cell are used on the same day.) [74]

After aliquotation transformation can be performed. DNA was added to the cells (1 µg DNA / 50 µl cells) and the suspension was mixed well. A six fold volume of 40%PEG/1xLiAc/0.5TE was added. The suspension was incubated at room temperature for 30 min. Dimethyl sulfoxide (DMSO) was added to a final

concentration of 10%. The suspension was then subjected to heat shock of 42°C for 20 min. The cells were sedimented for 3 min at 2,000 rcf. The supernatant was removed; the cells were resuspended in 100 µl H_2O and plated on selection plates.

3.3. Clonogenic Survival Assay

The clonogenic survival assay (CSA) is a basic method to test for cell death in yeast. To determine the percentage of colony forming units (CFU) at specific time points two dilution series (1:100 and 1:10,000) of the culture were prepared and the cell density (cells/ml) was measured by an automatic cell counter (CASY, Schärfe Systems). The first dilution was mixed into 10 mL CASYTON solution, containing 0.9 mM NaCL and 0.1 mM EDTA, resulting in a 1:10,000 final dilution. The second dilution was used to plate the equivalent of 500 cells on YPD agar-plates. After two days of incubation at 28°C, colonies were counted automatically by the colony counter of Lemna Tec.

In this study alls CSA experiments were performed twice as tetramer replicates. The cells were grown for 20h after lipid stress induction.

3.4. Lipid stress induction

Lipid stress was induced by DOG addition to the liquid medium. Unless otherwise stated, stress experiments were performed alike in either triplicates or quadruplicates. Cells were inoculated over night in SMD and grown to the stationary phase. The test sample was inoculated to OD_{600}=0.05 in selective medium, grown for 4 hours 15 minutes and treated with 1.45mM DOG dissolved in AcN. Control samples were treated with AcN only. Cells were further incubated for different amounts of time depending on the following experiment.

3.5. Microscopy

3.5.1. Sensing molecules

To examine DOG internalization and movement several sensing molecules were used (Table 2). These include a GFP-tagged PS sensor [8], a GFP-tagged $PI4,5P_2$ sensor [73] and a GFP-tagged DAG sensor [76]. The PS sensor was used to observe changes in the membrane structure and possible rearrangement due to non-physiological lipid surplus by DOG addition. The $PI4,5P_2$ sensor was used to track $PI4,5P_2$, one of the cellular DAG sources, upon DOG addition. The DAG-sensor was used to visualize movement of DAG and resulting changes due to DOG administration.

The PS sensor consists of the bovine lactadherin C2 protein domain that binds PS with high specificity and an N-terminal GFP-tag. Lactadherin is a milk glycoprotein that binds PS in a Ca^{2+} independent manner. The binding motif is localized to its C2 domain. The $PI4,5P_2$ sensor consists of two PH domains of the PLCδ protein of *Rattus norvegicus* and an N-terminal GFP-tag. PH domains are quite ubiquitous, present in numerous cell signalling proteins and display a wide range of PI-binding specificities. The PH domain of PLCδ is highly specific for $PI4,5P_2$. The DAG sensor consists of the murine PKD protein domain C1ab and an N-terminal GFP-tag. C1ab of PKD resulted in higher sensitivity for DAG than the previously used C1a domain of PKCγ. [76]

Each sensor was provided on a different plasmid (Table 2) with either URA (PS and $PI4,5P_2$) or HIS (DAG) selection marker. The plasmid was transformed into the strains of interest and subjected to microscopy. Strains only carried one plasmid at a time.

3.5.2. Microscopy and digital enhancement

After incubation for the allotted time the cells were harvested either by centrifugation (10,000 rcf, 2 min) or by mounting directly on agar slides and submitted to microscopy on a ZEISS Axioskop microscope using a Zeiss Plan-Neofluar objective lens with 63x magnification and 1.6x numerical aperture in oil (using Zeiss

Immersol) at room temperature. Fluorescence microscopic sample images were taken with a Diagnostic Instruments camera (*Model: SPOT 9.0 Monochrome-6*), acquired and processed using the Metamorph software (*version 6.2r4, Universal Imaging Corp.*). Digital enhancement was performed using ImageJ (v1.50). [77, 78, 79]

3.5.3. Cell cycle synchronisation

To achieve cell cycle synchronisation a *bar1Δ* strain was used [80]. To visualize DAG movement the DAG sensor plasmid was transformed. (Table 1, Table 2)

Cells were grown over night in SMD-HIS, inoculated to OD_{600}=0.2 and grown to OD=0.6 before harvesting (3,000 rcf, 3 min, RT). The supernatant was discarded; the pellet was washed in H_2O and resuspended in SMD-HIS containing 50 ng/ml α-factor.

Cells were then grown, while being checked for cycle arrest at 60, 90 and 120 min microscopically. After 120 min cell cycle arrest was observed in most cells, thus arrest was released by spinning and 2x washing. The pellet was then resuspended in SMD-HIS containing 50µg/ml nagase. The samples were then (without centrifugation) subjected to microscopy on agar slides every 20 min for 2 hours. [80]

3.6. Statistical analysis

Survival plating was performed in triplicates or quadruplicates. Raw data was tested for Gaussian distribution by Shapiro-Wilk test. Further analysis was performed by two-factor ANOVA, effectively comparing the differences between control and stress sample of a single knockout to the wild type. Programs used were SPSS 22, GraphPad PRISM 5.01 and Microsoft Excel 2013.

4. Results

4.1. Prevention of DOG induced cell death

4.1.1. Knockouts of *vps34Δ* and *snf7Δ* prevent cell death

CSA of *vps34Δ*, *vps24Δ* and *snf7Δ* was performed as described in section 3.3 in quadruplets in two separate experiments. The knockouts of both *vps34Δ,* encoding the PI3K, and *snf7Δ,* coding for the ESCRT-III assembly subunit, show significantly better survival faced with DOG induced lipid stress than the wild type BY4741. On the other hand *vps24Δ,* coding for the ESCRT-III disassembly handle, behaves similar to the wild type. (Figure 4)

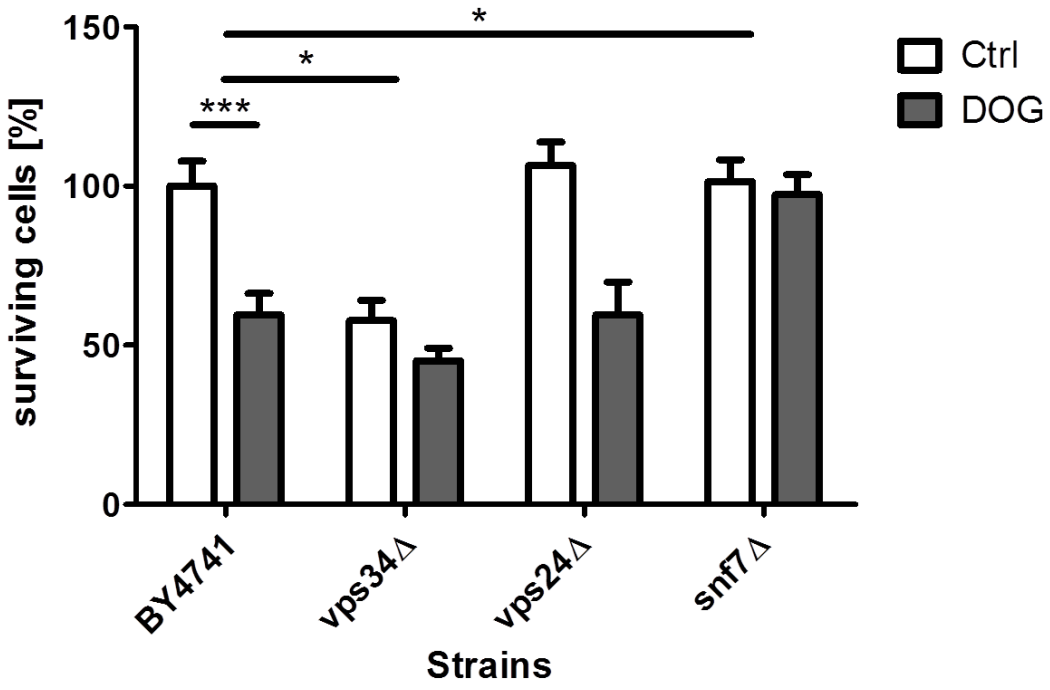

Figure 4: Clonogenic survival assay of endosome-associated proteins with DOG induced stress. Y-scale depicts surviving cells in percent. 100% is set to wild type control. White bars represent control samples, grey bars represent lipid stress samples. Asterisks indicate statistical significance tested by two-way-ANOVA. ($p < 0.05$ *, $p < 0.01$ **, $p < 0.001$ ***) Error bars represent standard error mean.

4.1.2. Knockouts of SNARE-proteins prevent cell death

The CSA of the non-essential SNARE proteins, Vam3 and Vam7, as well as the corresponding Rab-GTPase Ypt7 was performed in the same way as above. Interestingly, all tested knockouts prevented DOG induced cell death. (Figure 5)

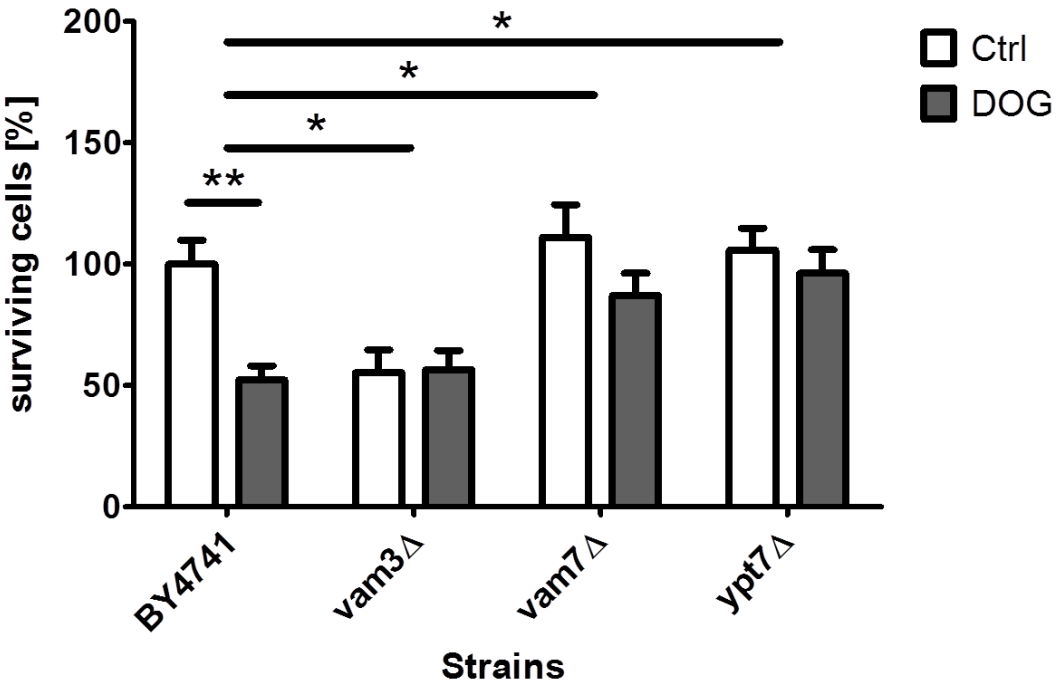

Figure 5: Clonogenic survival assay of non-essential SNARE proteins with DOG-induced stress. Y-scale depicts surviving cells in percent. 100% is set to wild type control. White bars represent control samples, grey bars represent lipid stress samples. Asterisks indicate statistical significance tested by two-way-ANOVA. ($p < 0.05$ *, $p < 0.01$ **, $p < 0.001$ ***) Error bars represent standard error mean.

4.1.3. Knockout of *ypt32Δ* prevents cell death

The CSA of deletion strains of the two tested Rab GTPases associated with the recycling endosome showed that only *ypt32Δ* prevented cellular demise induced by DOG. (Figure 6) Ypt31 and Ypt32 are supposedly paralogues. The double knockout of these is lethal and could thus not be tested. [72] The CSA was conducted in quadruplicates and performed three times.

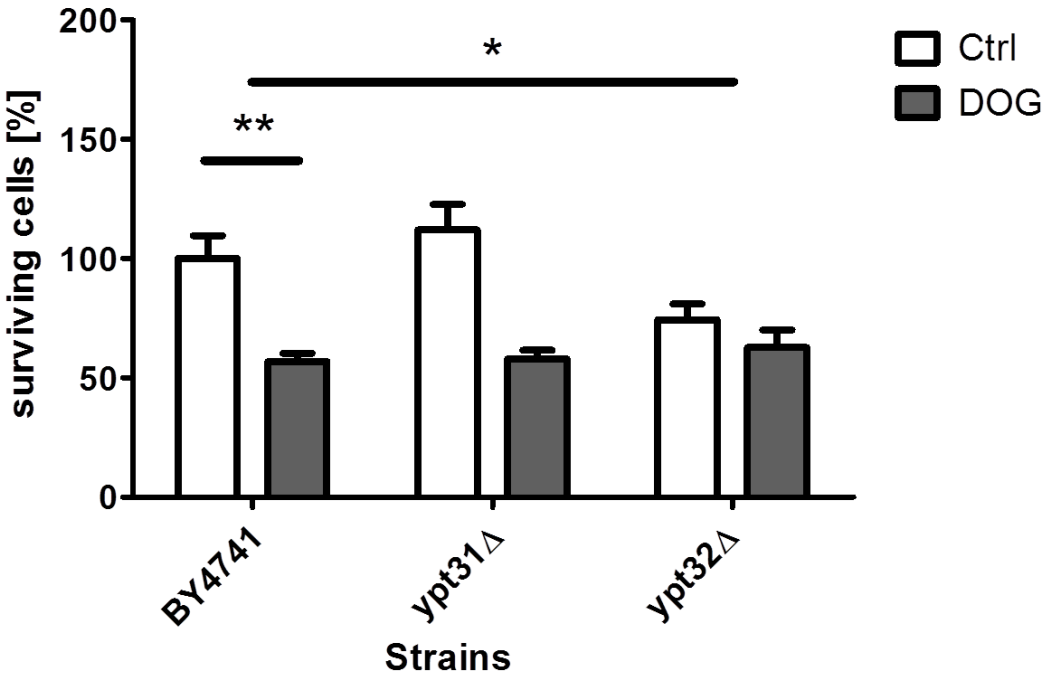

Figure 6: Clonogenic survival assay of RE-associated Rab-GTPases with DOG-induced stress. Y-scale depicts surviving cells in percent. 100% is set to wild type control. White bars represent control samples, grey bars represent lipid stress samples. Asterisks indicate statistical significance tested by two-way-ANOVA. ($p < 0.05$ *, $p < 0.01$ **, $p < 0.001$ ***) Error bars represent standard error mean.

4.2. Microscopic localisation studies

4.2.1. The dynamic DAG distribution upon DOG administration

To examine the effects of DOG treatment on the cells DAG-distribution the wild type strain containing the DAG sensor plasmid was subjected to microscopy in a time course experiment (Figure 7). The series was started one hour after DOG addition. The control was treated with AcN solvent instead.

At the beginning (1h mark) there is no visible difference. Both control and DOG sample show a GFP signal at the VM accompanied by some cytosolic dots. At the 2h-mark DOG starts giving rise to a GFP signal at the PM, while the control does not. Cytosolic dots grow in size in both samples. The VM signal is stronger in the control than in the DOG sample. At the 3h-mark the control begins to show slight PM signal, although the majority remains at the VM as well as the cytosolic dots.

The DOG sample shows a more intense signal at the PM with little to no signal from the VM. The cytosolic dots are fewer than in the control. At the 4h-mark the control shows good PM signal equal to the DOG sample. The cytosolic dots of the control persist and those of the DOG sample increase to ctrl levels. VM signal is still stronger in the ctrl. At the 5h-mark the VM signal is barely detectable in the control and in the DOG sample. Both samples give good PM- and cytosolic dot-signals. There is only little difference. At the 6h-mark the signal is the same as after 5h.

We then switched to longer intervals of 2h. After 8h there is no difference again. Both samples show signal at PM and some cytosolic dots. At the 10h mark movement is observed in the control sample, whereas the DOG sample remains unchanged at that time point. The control shows weaker PM signal, with dots as well as a homogenic cytosolic signal. At the 12h mark the control shows vacuolar signal again in addition to the signals visible after 10h. The sensor appears to translocate to the vacuole where it is internalised, as both VM and vacuolar lumen are GFP-positive. The DOG sample however shows no difference compared to 8 and 10h. After 14h the Ctrl shows more distinct vacuolar signal, while the DOG sample does not change at all.

Finally, the last point of the series was set to 21h. At this time the control shows massive signal inside the vacuole. There is little signal at the PM and few weak cytosolic dots. The DOG sample however shows strong PM signal and no vacuolar signal at all. (Figure 7)

4.2.2. DAG moves from mother to daughter cell in large amounts via vesicles originating from the vacuole

To test whether the observed DAG movement was somehow related to the cell cycle we examined synchronisable cells of the *bar1Δ* genotype. First the cell cycles were synchronised (Section 3.5.3) and DAG signal was observed during the synchronisation phase (Figure 8a). After homogeneity and cell cycle arrest was achieved in the majority of the cells, the arrest was released and DAG movement was closely observed (Figure 8b).

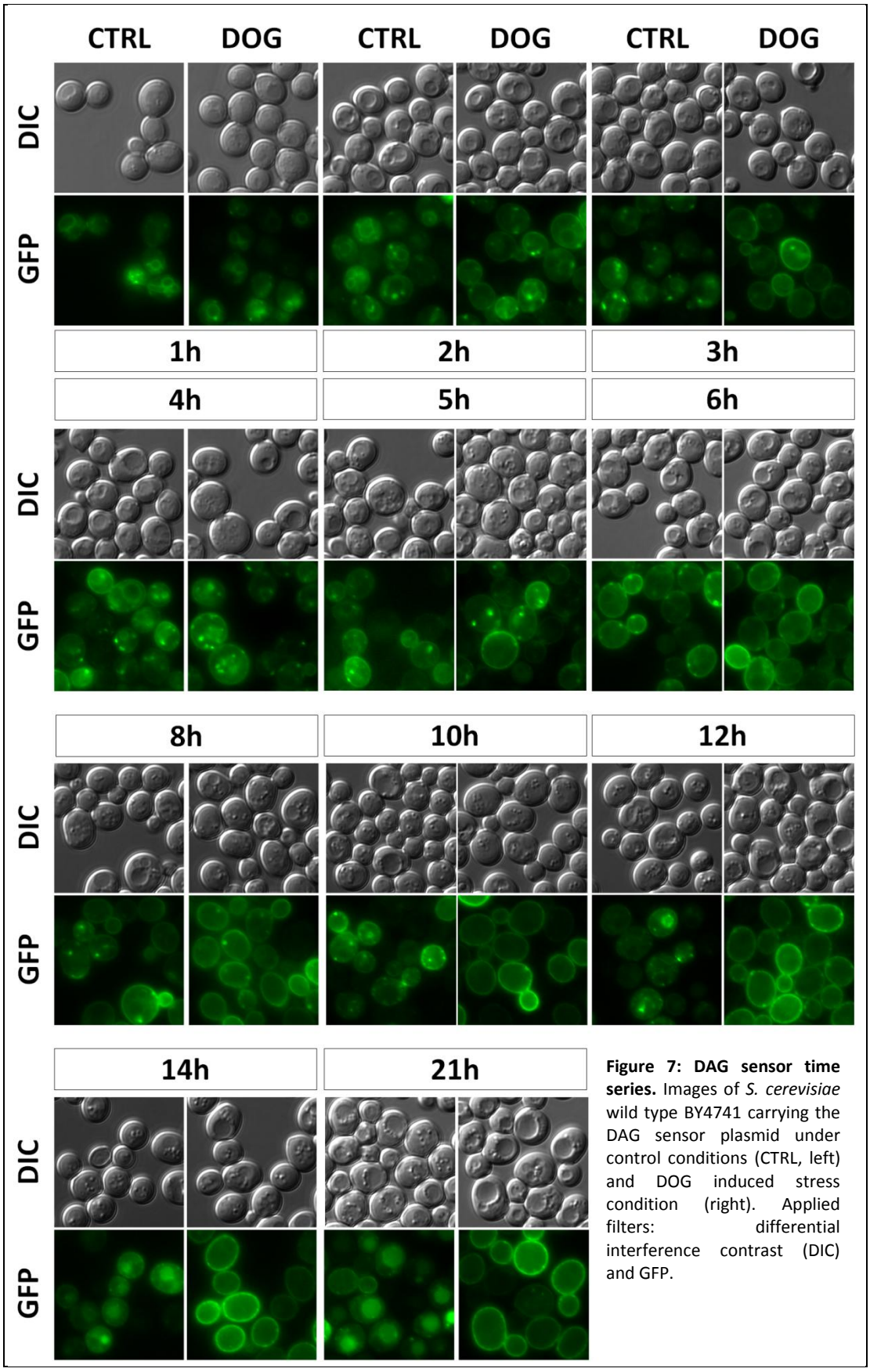

Figure 7: DAG sensor time series. Images of *S. cerevisiae* wild type BY4741 carrying the DAG sensor plasmid under control conditions (CTRL, left) and DOG induced stress condition (right). Applied filters: differential interference contrast (DIC) and GFP.

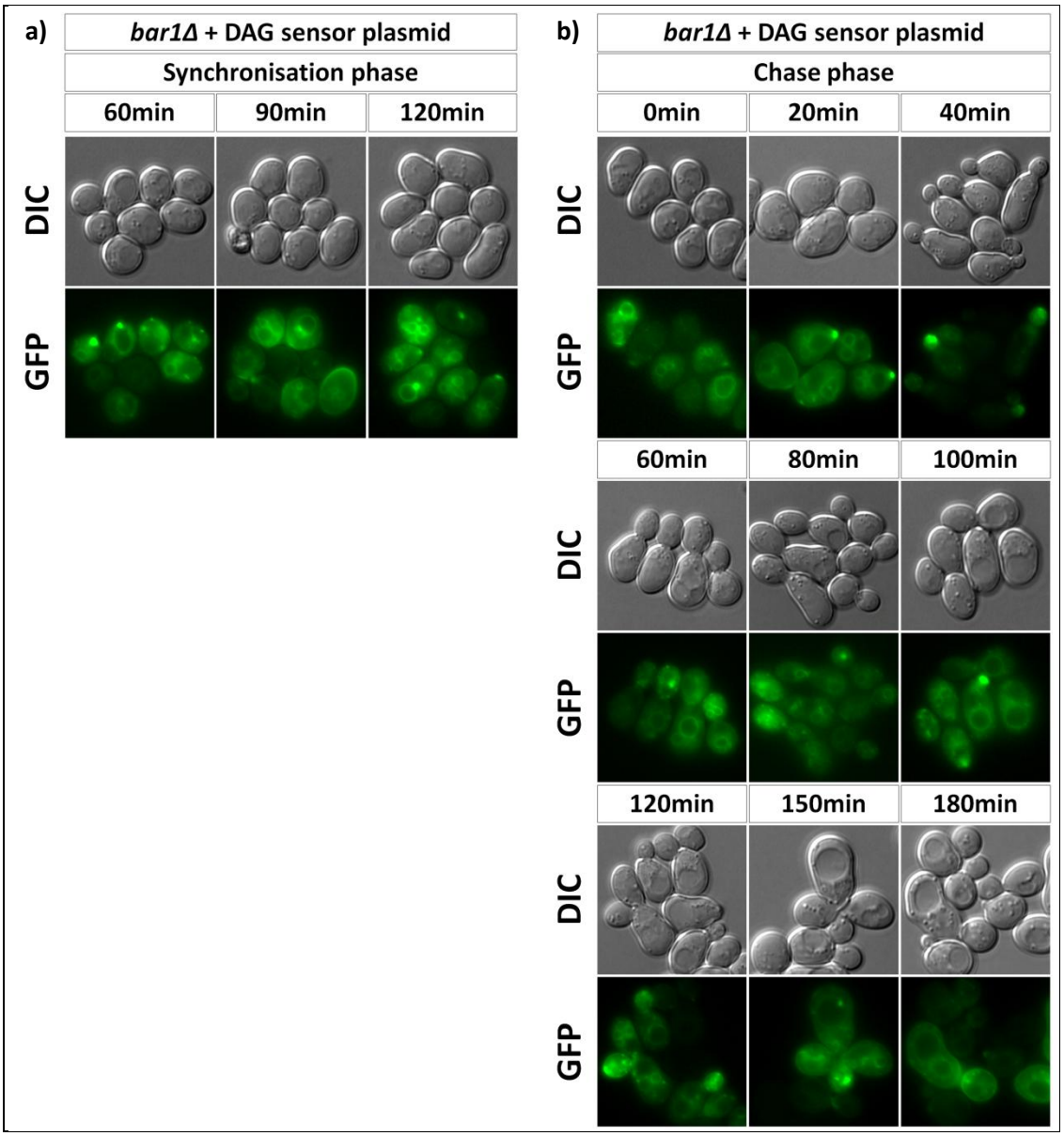

Figure 8: DAG sensor during cell cycle synchronisation (a) and after cycle arrest release (b). Images of *S. cerevisiae bar1Δ* carrying the DAG sensor plasmid under control conditions. Applied filters: DIC and GFP.

During synchronisation phase DAG can be observed at the VM at all times and also in cytosolic dots at the PM. The dots then move to the vacuole showing little remaining cytosolic signal (Figure 8a). Predominant VM signal turns out to be the link to the chase phase.

After cycle arrest release the DAG moves from the VM to the growing bud, while the cytosolic signal suggests formation of DAG containing vesicles (Figure 8b, 20 min). After 40 min the signal is predominantly detectable at the growing bud with little to no signal from the mother cell. Upon formation of the daughter cell (60 min)

the VM signal is clearly visible in both the mother and daughter cell. The daughter cell additionally shows signal from the ER or a pre-vacuolar compartment and dots at the PM, which before were only visible in the synchronisation phase. After 80 min the signal is mostly at the VM with few cytosolic dots in the daughter cell. After 100 min the cells have completely separated. The DAG-localisation is identical for mother and daughter cell at VM and dots close to it. The 120 min mark shows no change. After 150 min movement to the PM would have been expected, but it is only visible after 180 min.

4.2.3. PI4,5P_2 localisation shows little difference upon DOG addition

PI4,5P_2 is the main PIP of the PM. We wanted to track the cellular PI4,5P_2 distribution using the corresponding sensor (section 3.5.1) under both control and DOG stress conditions. We hypothesised that DOG stress induced endocytotic budding of the PM. The control sample was treated with AcN as before. The time series was performed in 2h steps after DOG addition up to 20h with additional early time points at 1h and 3h (Figure 9). Propidium iodide, a membrane impermeable and intercalating agent, was used to stain necrotic cells (red signal).

The control sample shows PM-localisation at the beginning. At 2, 3 and 4h the localisation changes to the cytosol with sporadic accumulations (mostly a single one). After 6h the cytosolic signal is very weak, but the PM signal is strong again and persists until 20h. At 8h there is again more cytosolic signal and dots appear at the PM, which still gives a strong signal. These dots are hardly visible after 10h, but appear at all later time points except for 20h, most distinctly after 12h and 14h. The cytosolic signal appears to increase after 16h but decreases again at 18h. After 20h there is a large fuzzy accumulation close to the vacuole.

The DOG-sample starts out differently than the control. The signal at the PM appears weaker, in contrast to the ample cytosolic signal at the 1h-mark. At 2h there is less PM signal and dots appear close to the PM. At 3h there is no difference to the control, both show cytosolic signal only. From 3h to 8h there is no change in the signal, which is only cytosolic. At 10h the signal at the PM is strong again, with some cytosolic signal remaining. From 12h to 18h the PI4,5P_2-signal does not differ

from the control sample and shows a PM signal with dots and some cytosolic signal. After 20h however, there is a difference again, as the DOG-sample shows still the same as before without the fuzzy accumulation from the control.

Notable differences upon DOG addition are the early appearance of cytosolic accumulations and their persistence as well as the delayed PM signal, and the lack of the prevacuolar compartment.

4.2.4. DOG induced changes in PS localisation in wild type cells and *rim13Δ* differs in the time course.

The distribution of PS was examined due to its potential of being a DOG responsive handle in the PM involved in DOG cell entry or transport.

S. cerevisiae wild type and *rim13Δ* cells carrying the PS sensor plasmid (section 2.1, Table 2) were examined in a time course experiment with and without addition of DOG resulting in a time series akin to DAG sensor and PI4,5P_2 sensor. At the early time points (2-6h) in the series there is hardly any difference caused by the strains or the growth conditions (Figure 10). PS predominantly localises to the PM as expected and there are indications of transportation to the VM via vesicles.

At the later points of the series (12-16h) differences in PS localisation start to appear (Figure 11). At the 12h mark the wild type shows PS at the PM in the control sample, while the DOG sample still shows some signal at the VM. The *rim13Δ* knockout control sample is similar to the wild type. The DOG sample however shows PS accumulation close to the vacuole. After 14h the wild type control predominantly shows PS at the PM, but also some faint homogenic cytosolic signal. The DOG sample however shows distinct accumulation at the VM. Similarly the *rim13Δ* control sample shows signal at the PM as well as in the cytosol. The *rim13Δ* DOG sample however shows fuzzy accumulation again. At the 16h mark the difference between control and DOG samples are most distinct. The wild type shows PS at the PM in both samples, but VM and prevacuolar accumulations only in the DOG sample. The *rim13Δ* knockout shows signal at the PM in both samples, but only the DOG sample shows fuzzy prevacuolar accumulations as well as some dots at the VM. Thus the 16h mark was chosen for examination of further knockouts.

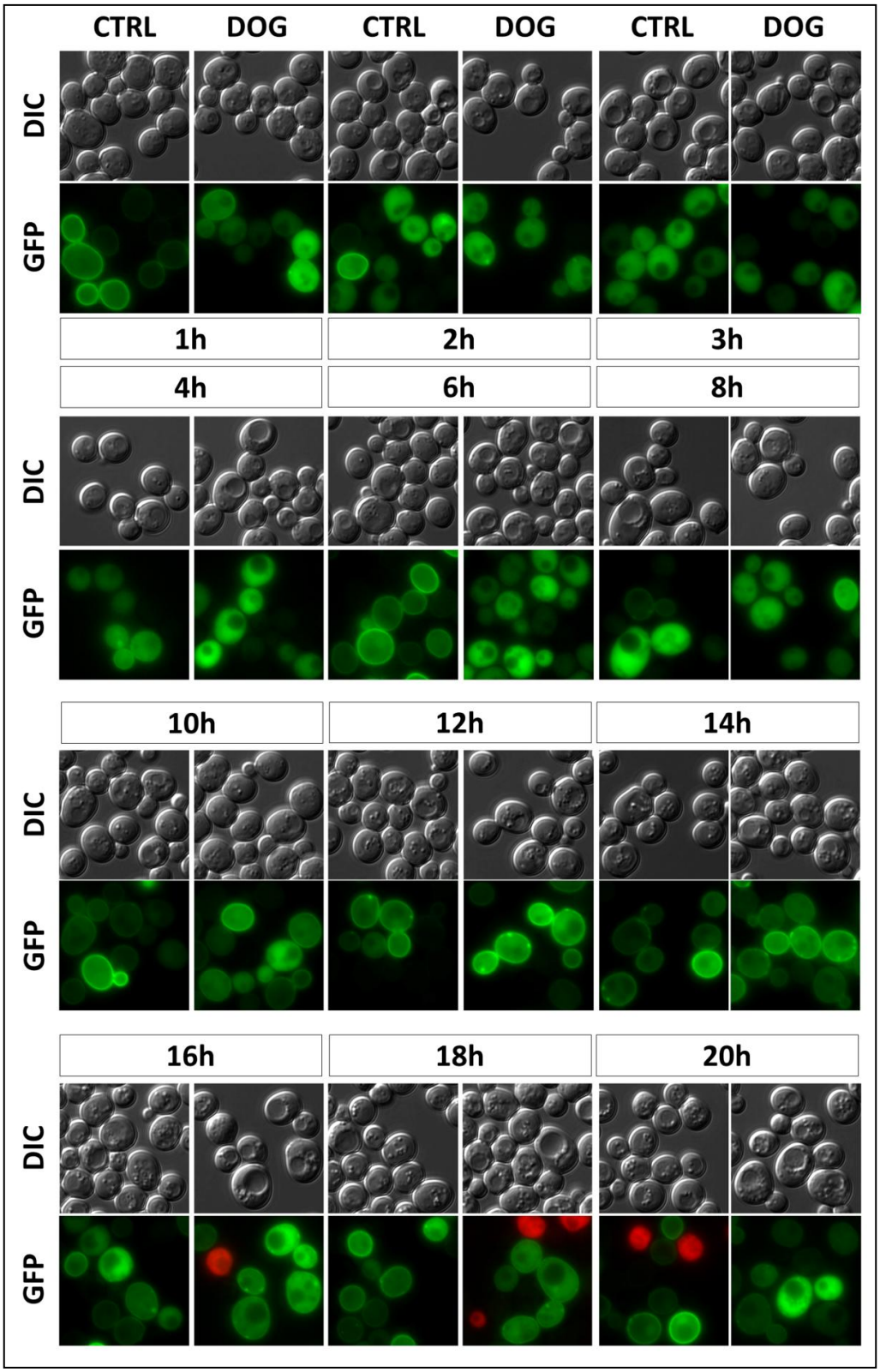

Figure 9: PI4,5P2 time series. Images of *S. cerevisiae* wild type BY4741 carrying the PI4,5P2 sensor plasmid under control conditions (CTRL, left) and DOG induced stress condition (right). Applied filters: DIC, GFP and dsRed.

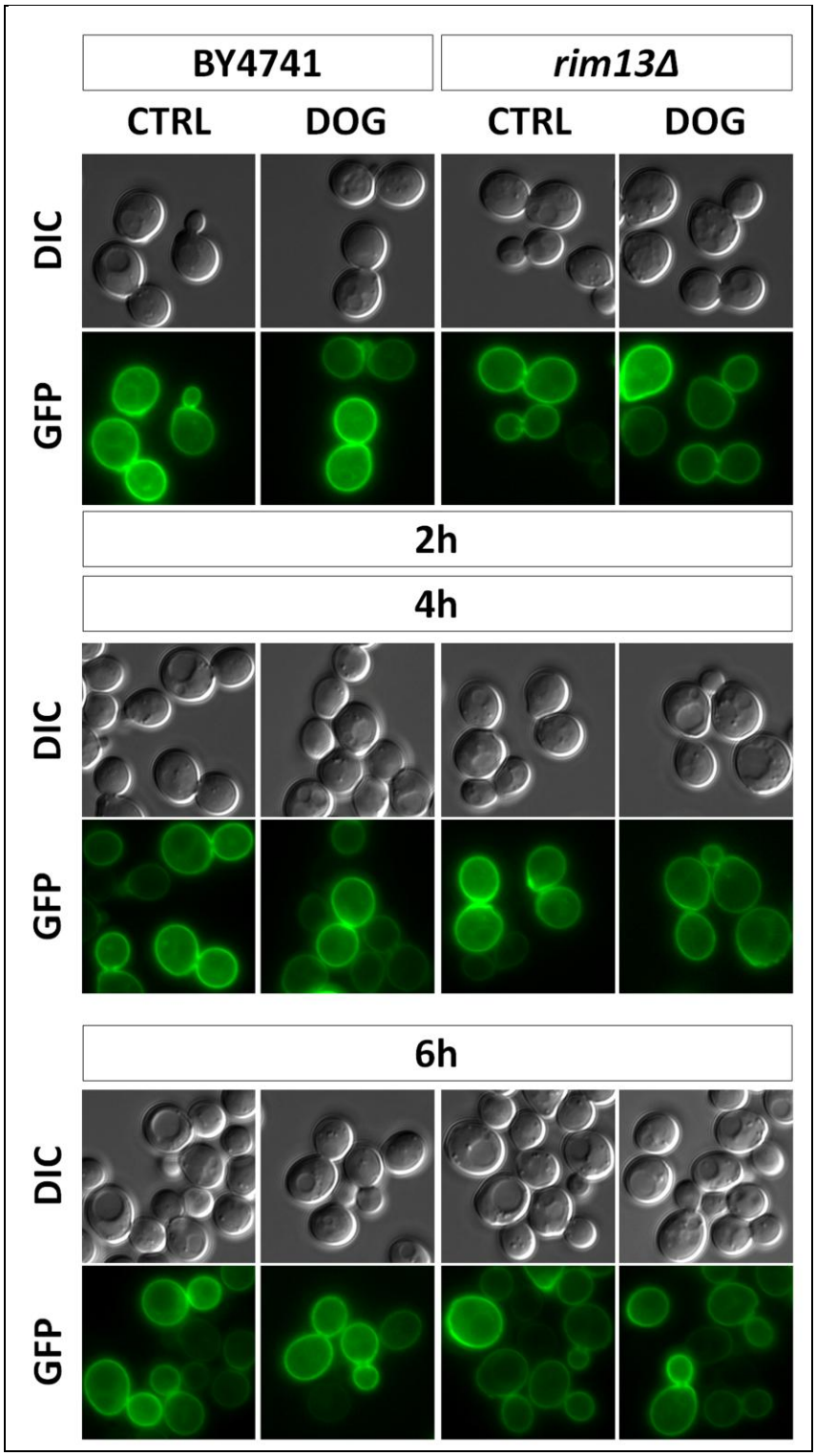

Figure 10: PS sensor time series 2-6h. Images of *S. cerevisiae* wild type BY4741 (left) and *rim13Δ* (right), each carrying the PS sensor plasmid under control conditions (CTRL, left) and DOG induced stress condition (right). Applied filters: DIC and GFP.

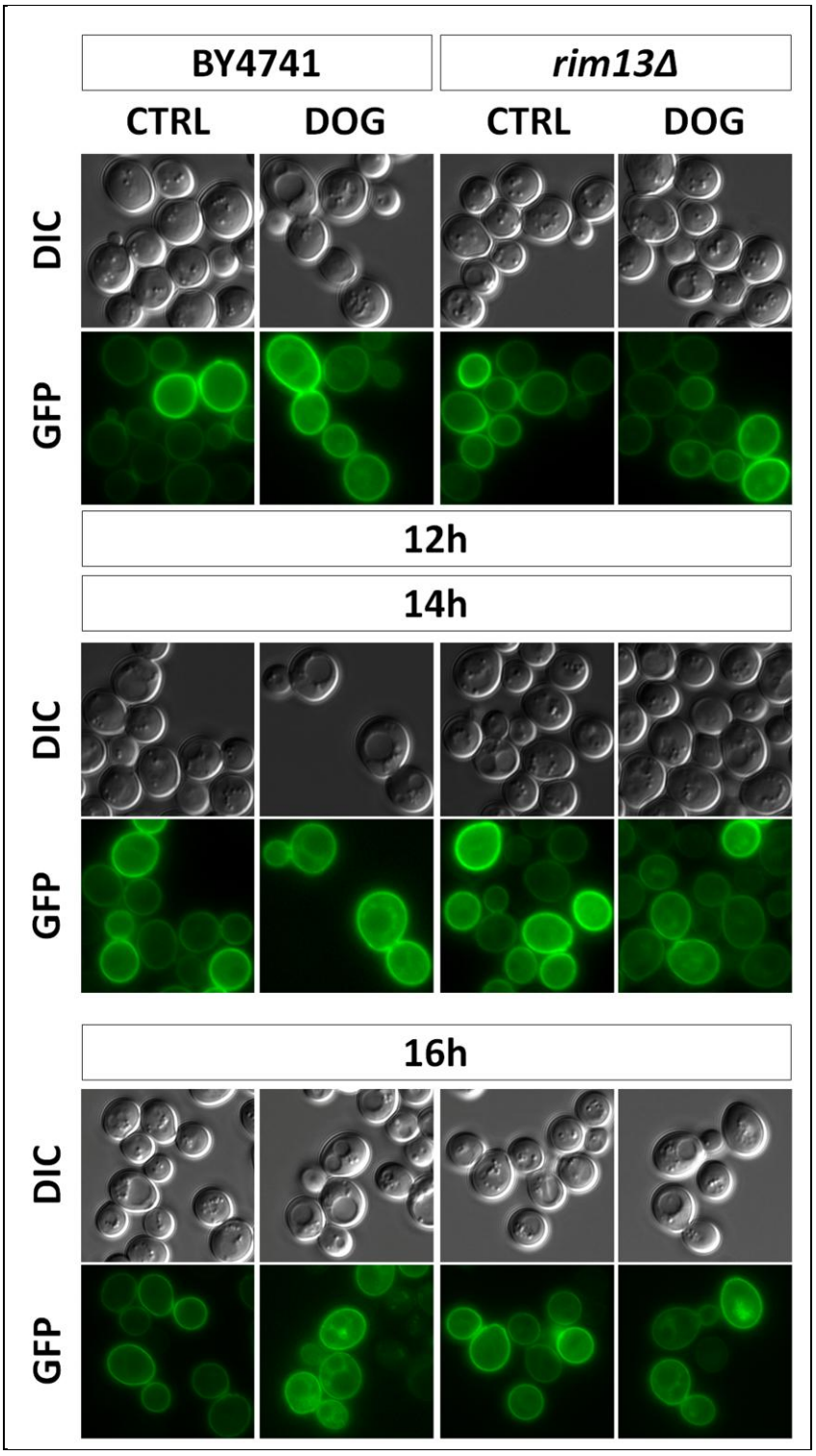

Figure 11: PS sensor time series 12-16h. Images of *S. cerevisiae* wild type BY4741 (left) and *rim13Δ* (right), each carrying the PS sensor plasmid under control conditions (CTRL, left) and DOG induced stress condition (right). Applied filters: DIC and GFP.

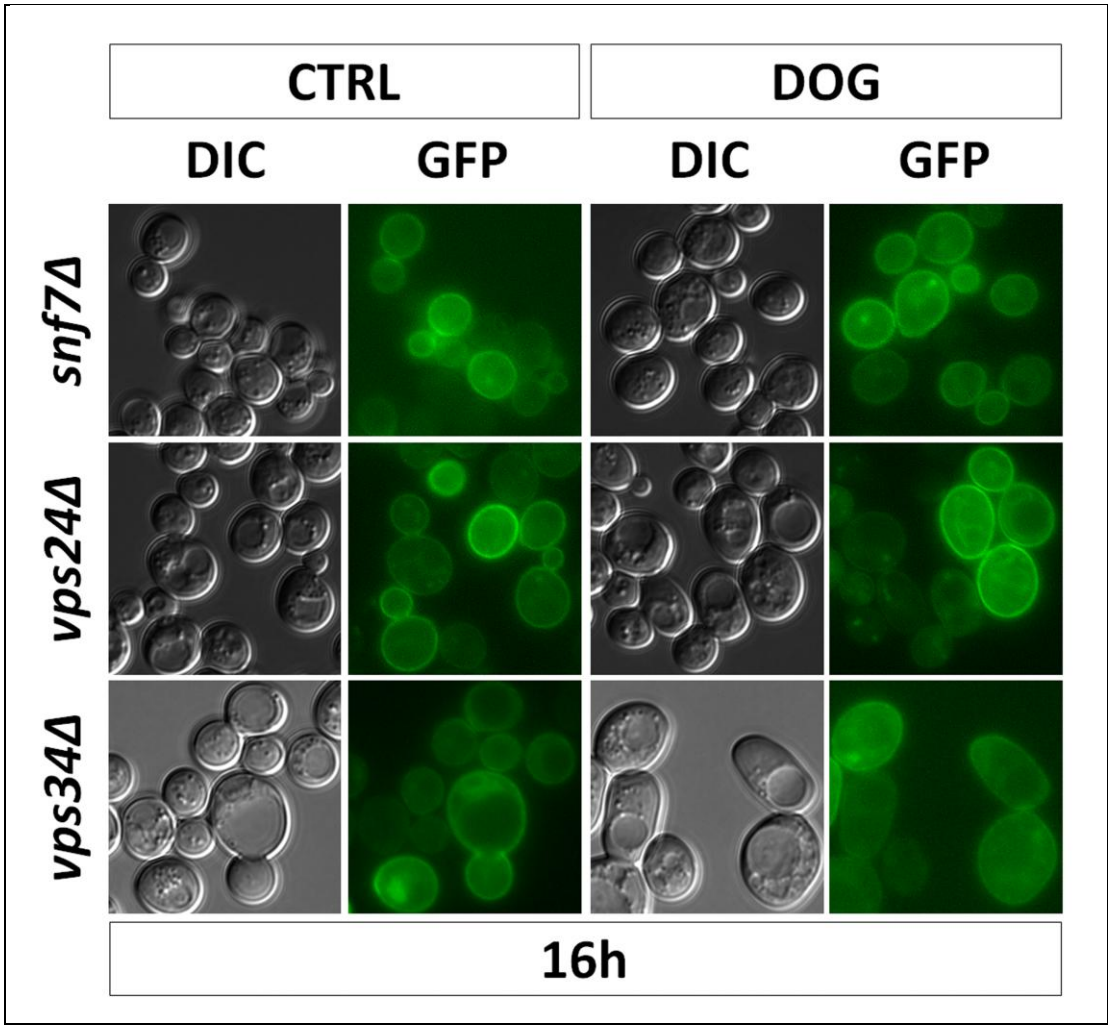

Figure 12: PS localisation in class E and class D vacuolar morphology. Images of *S. cerevisiae snf7Δ*, *vps24Δ* (both class E) and *vps34Δ* (class D), each carrying the PS sensor plasmid under control conditions (CTRL, left) and DOG induced stress condition (right). Applied filters: DIC and GFP.

4.2.5. DOG induced changes of PS localisation in vps-gene knockouts of the same class differ.

The class E vacuolar morphology associated knockouts of *snf7Δ (vps32Δ)* and *vps24Δ* show different phenotypes as expected due to the results of the corresponding clonogenic survival assay (section 4.1.1, Figure 4). Wild type like behaviour appears in the *snf7Δ* control sample with mostly localisation to the PM, but also some cytosolic accumulations. The DOG-treated sample however shows more and stronger cytosolic accumulations than the untreated sample, but does not reach the level of the wild type DOG sample. Apparently the effects are less severe than in the wild type. The *vps24Δ* knockout behaves differently. The obligatory PM signal is also present

here, while there are cytosolic dots already appearing in the control sample. There is only mild VM signal, but both dots and VM signal are increasingly visible in the DOG-treated sample. The class D associated knockout of *vps34Δ* shows little to no difference in PS localisation due to DOG stress at all. Both samples show PM signal and prevacuolar accumulation of the sensor, which might be decreasing upon DOG addition (Figure 12).

5. Discussion

5.1. DOG induced cellular demise requires the endosomal pathway

Involvement of the endosome in DOG associated cellular demise is suggested by the effects observed in the knockouts of the ESCRT-III components Snf7 and Vps24 (section 4.1.1, Figure 4). Snf7 and Vps24 promote antagonistic behaviour of the ESCRT-III complex [84]. The subunit consisting of Snf7 and Vps20 mediates complex assembly and enables the Rim13-dependent cleavage of the transcriptional repressor Rim101. Vps24, paired with Did4, on the other hand mediates complex disassembly via the AAA-ATPase Vps4. Thus the genetic knockout of *snf7Δ* causes artificial inactivation of the ESCRT-III complex impairing both Rim101 cleavage as well as endosomal trafficking. The *vps24Δ* knockout causes adverse effects in the form of a constitutively activated ESCRT-III complex unable to disassemble. [84] Prevention of DOG induced cell death by *snf7Δ* and failure of the same by *vps24Δ* suggests that impairment of endosomal transport and protein sorting plays a major role in DOG-induced lipotoxic cell death. Further support comes in the form of cell death prevention by the knockout of the PI3K gene, *vps34Δ* (Figure 4). PIPs are key molecules serving as either structural or membrane molecules or precursors to the water soluble IPs. PI3P specifically appears as part of the endosomal membrane and MVBs. Thus the knockout of the only PI3K leads undoubtedly to a shortage of PI3P and thus impairs endosome formation, trafficking, protein sorting and maturation. PI3P also serves as a precursor of $PI3,5P_2$, a PIP that is mostly located to the VM. PI3P shortage thus also leads to $PI3,5P_2$ decrease and further impairs fusion of MVB and vacuole.

5.2. Impairment of vacuolar SNARE proteins prevents DOG induced cell death

The global approach of PIP regulation tends to bring along some side effects. To further narrow down the DOG effect to the endosomal pathway SNARE proteins mediating the MVB/vacuole fusion were examined. Impairment of the SNARE leads

to significantly better performance in the clonogenic survival assay (section 4.1.2, Figure 5). The genes coding for the R- and Q_B-SNARE proteins are essential, thus we decided to test the genetic knockouts of Q_A- and Q_C-SNARE proteins (Vam3, Vam7) as well as the corresponding Rab-GTPase Ypt7. All of the tested knockouts showed prevention of the DOG induced cell death. Removing a single SNARE protein causes inability of SNARE formation due to its complex structure [85]. The selected knockouts show differences in survival at control conditions as well, such as the overall low viability of *vam3Δ*. Despite its decreased viability *vam3Δ* does not falter upon DOG application. Thus the affected pathway appears to be essential for DOG induced cellular demise.

5.3. The two yeast paralogues of Rab-GTPases of the recycling endosome affect cell death differently

Ypt31 and Ypt32 are Rab-family GTPases located to the recycling endosome serving as its biomarker [72]. DOG might be degraded in the vacuole, but its product octanoic acid still remains non-physiological in yeast. As such its further metabolism is of interest. The recycling endosome provides the shuttle for octanoic acid to other organelles such as the Golgi or ER. In all likelihood the deletion of one of the paralogues Ypt31 and Ypt32 should result in similar effects, yet they do not. Genetic knockout of *ypt31Δ* has no effect on DOG induced cell death, while *ypt32Δ* convincingly prevents cellular demise (section 4.1.3, Figure 6). This difference can be attributed to two features protein amount and cellular metabolism. First, the protein levels of these Rab-GTPases might largely differ. At least for DNA replication stress it has been reported that Ypt32 levels are highly increased. [81] Along these lines, DOG might interfere with Ypt32 up-regulation thus preventing Ypt32 of keeping the cell alive via a mechanism that is not available to Ypt31. Also the slightly higher isoelectric point of Ypt32 might play a role in response to DOG. The differing effects of these paralogous proteins remain unclear. Secondly, the *ypt32Δ* knockout already shows decreased viability in the control sample. The saving effect of *ypt32Δ* may be less associated with detrimental effects of the combination

of DOG and Ypt32 but rather to the slower metabolism of the mutant cells, thus delaying DOG induced cell death.

5.4. DOG application impairs cellular DAG recycling and may repress further membrane associated processes

Under standard conditions DAG first locates to the VM and accumulates in cytosolic dots. With time the cytosolic dots increase in size and the signal locates at the PM. After DAG reaches the PM, the vacuolar fraction decreases, while the PM fraction increases with stable cytosolic accumulations. (1-8h) Depending on the cell cycle the signal retreats from the PM and moves to the VM, while cytosolic accumulations increase in number. Contrary to the early time points the signal changes to the vacuole instead of remaining at the VM. The PM signal decreases below the detection threshold, while cytosolic accumulations decrease in both size and number. (Figure 7)

The cell appears to distribute DAG from LDs with the help of enzymes located to the VM. When the cell cycle progresses, DAG moves to the PM via vesicles in preparation of membrane restructuring prior to mitosis. While the PM fraction grows stronger the VM fraction weakens suggesting that DAG levels decrease on the VM. The cytosolic accumulations, most likely LDs, increase in size over time suggesting that newly produced DAG is directly shuttled from the LDs to the PM. When the cells near the stationary phase, the PM signal decreases and cytosolic accumulations increase in number but decrease in size. Apparently DAG is moved from the PM to the vacuole via the endosomal route, while the signal from LDs decreases in size due to the lower DAG amounts present. The constant restructuring of the PM leads to removal of DAG from the PM and subsequent degradation in the vacuole. At the PM DAG might be further processed in a way that disables binding of the sensor molecule, causing it to be moved to the vacuole for degradation. The vacuolar signal most likely only represents the GFP-barrel of the sensor molecule. The complex of DAG and sensor might be disassembled at the PM and if not there then in the

vacuole due to protein denaturation and degradation. The barrel form of GFP degrades slower than most proteins including the C1ab domain of the murine PKD.

The cycling of DAG from the VM and LDs to the PM and subsequent incorporation into the membrane is disturbed by DOG addition due to either the massive amount being supplied or the methods of yeast to deal with octanoyl residues being inefficient.

At the beginning, 1h after DOG addition, there is no difference to the control situation. DAG locates to the VM and cytosolic dots. Shortly later the DOG addition causes signal at the PM, which appears faster than in the control. At the same time VM signal and cytosolic accumulations weaken substantially upon DOG stress. The cytosolic accumulations appear again, but the VM is not stained anymore. From the 2h mark onwards the constantly strongest signal in the DOG sample comes from the PM. At the time the control sample starts to redirect DAG from the PM to the vacuole, the signal stays firmly planted at the PM in the DOG sample. Minor dots appear on the PM, but there is no evidence at all to support trafficking of DAG from the PM to the vacuole akin to the control sample. (Figure 7)

It appears that the addition of non-physiological DAG-species hinders the cells membrane shuffling and thus impairs processes depending on membrane restructuring such as mitosis, endocytosis, mating and response to external force.

5.5. DAG distribution during cell cycle

During cell cycle arrest DAG seems to locate to the VM and also structures located in close proximity to the VM, which might represent the ER or LDs. Localisation to the growing bud was only a rare event. (Figure 8a)

The synchronised growth after release of cell cycle arrest clearly shows DAG movement originating from the VM and cytosolic structures nearby: probably ER and LDs. We hypothesize that upon mitosis induction the DAG moves to the growing bud via vesicle trafficking. The lack of DAG signal from the mother cell upon bud formation suggests that the majority of synthesised DAG is moved to the

bud to establish the daughter cell. Once the daughter cell is more clearly formed, DAG signal increases in the mother cell as well. Apparently, DAG synthesis is increased to satisfy the demand. During cell formation the DAG signal is not limited to vacuole or LDs, but spread to all compartments requiring DAG, which may include Golgi and ER as well as the nucleus and mitochondria. Closing in on completion of the cell division the DAG signal once again originates from the VM and cytosolic dots, which is maintained after separation of daughter and mother cell. About fifty to eighty minutes after separation the cells show DAG signal at the PM in addition to the VM and LDs. Ample PM signal can be expected in every cycle during PM synthesis, yet there is no PM signal at either 80 or 100 minutes. Anyhow, there are accumulations close to the PM, suggesting that the clear PM signal was missed and maybe occurred at about 90 minutes. The repeated formation of bright dots near the vacuole may indicate fusion events with the VM. (Figure 8b)

5.6. PI4,5P_2 localisation upon DOG addition indicates hastened cellular demise possibly caused by ER transport blockage

The PM associated PI4,5P_2 shows initial localisation to the membrane as expected, but soon the cytosolic signal takes over (Figure 9). The homogeneity of the cytosolic signal begs the question, if the sensor is still bound to PI4,5P_2 or if the incorporation at the PM disassembles the complex preventing the PLCδ-PH domain to bind its target. The recurring PM signal after six hours favours the complete dissociation of the sensor in complex with PI4,5P_2 and subsequent de novo synthesis of PI4,5P_2 by the membrane bound PI4P 5-kinase. The appearance of dots over time might be accumulations of newly synthesised PI4,5P_2 or aggregates ready for dissociation and following degradation. During stationary phase the dots are reduced in number and size until a single prevacuolar accumulation is formed.

The DOG treatment causes dots at the early time points already, although they vanish in favour of the homogenic cytosolic signal. Interestingly the PM signal is delayed in the DOG sample, which was only observed at the ten hours time point. Apparently,

DOG treatment slows the de novo synthesis of $PI4,5P_2$ at the PM via PI4P 5-kinase. Entering the stationary phase again the cells show dots located at the PM. These are interestingly more persistent than in the control and might indicate hastened cellular demise. The PM signal decreases in favour of the cytosolic signal compared to the control sample indicating disturbed PL distribution at the PM. Additionally, the prevacuolar accumulation does not appear in the DOG sample. The cellular site of accumulation might be the ER. DOG treatment might impair trafficking from the PM to the ER, thus disturbing lipid homeostasis. (Figure 9)

5.7. PS localisation reveals minor, possibly ER-related differences between wild type and death preventive RIM13 knockout

PS translocation was not observed at early time points in wild type cells. (Figure 10) This is within expectations. DOG-induced cell death only appears after about 12h. After 14h and 16h cellular demise becomes more prominent. 20h after DOG administration 50% of wild type cells have succumbed to cell death. Reshuffling of PS, a major PM component, in large amounts would cause loss of membrane integrity. Loss of integrity and the following instability may quickly lead to PM rupture and inevitable cell death in a necrotic manner. Thus the major PS relocalisation should appear shortly before cellular demise becomes obvious. PS signal at the VM and scattered cytosolic dots are within expectations as evidence of occasional trafficking processes.

The *rim13Δ* knockout similarly shows hardly any difference, with PS predominantly at the PM. Also there are faint signals from the VM and cytosolic accumulations. It appears that the PS metabolism is slowed down in the knockout in the early stages, since there are no cytosolic dots visible in the initial scan. However, the 4h and 6h marks hardly differ from the wild type. (Figure 10)

At the later, more pressing time points the DOG effect starts to develop. The wild type control features nearly exclusively PM localisation, concurrent with the shift to the stationary phase. The localisation in the DOG sample however suggests

continuous rearrangements with signal at the VM, cytosolic accumulations as well as PM signal. These differences are apparent from 12-16h increasing in distinctness in the later samples. Starting with faint VM signal, continuing to vivid dots at the VM and evolving into prevacuolar compartments these effects suggest that DOG induces PS trafficking and subsequent metabolism.

We expected different behaviour of PS localisation upon DOG addition in the *rim13Δ* knockout due to its preventive effect in the CSA (data not shown). However, the difference was not so obvious. The control samples of both strains do hardly differ in any time point. For the DOG sample the verdict is however different. Even at 12h fuzzy cytosolic accumulations - maybe the ER - are clearly visible. There is hardly any VM signal, which only appears at the 18h mark. The supposedly ER related signal remains visible from 12-16h and suggests much like the wild type sample increased PS metabolism. These results suggest, that DOG induces PS trafficking upstream of Rim13. Possibly, it prevents fusion of these PS containing vesicles with LDs and thereby inhibits delivery of DOG, thus preventing cell death (Figure 11). This hypothesis would explain for the persistence of PS vesicles in the knock out.

5.8. PS localisation in vps-gene knockouts does not coincide with CSA results

The PS localisation in the vps-gene knockouts brings some expected, but also unexpected results with it. The cell death preventing *snf7Δ* shows localisation similar to the wild type. The effects appear less distinct, with only minor cytosolic accumulations in the DOG sample, maybe derived from LDs. Similar to *rim13Δ* the difference of PS localisation in the DOG sample compared to the wild type is less extreme than expected. There appears to be no ER related signal in *snf7Δ* though. (Figure 12)

The counterpart to *snf7Δ*, *vps24Δ*, causes cytosolic accumulations and faint VM signal in the control sample. Apparently the constitutively assembled ESCRT-III complex causes intracellular PS localisation. Initially, we explained these dots as

being associated to the RE, but it turned out, that in wild type cells no colocalisation of PS and Ypt31-EBFP could be detected (Supplemental Figure 1). Ypt31 is the RE Rab GTPase, that we used as a biomarker. This begs the question, if these observed dots are of endosomal nature, LD derived or maybe fractions of other membrane types like ER, vacuole or even autophagosomes. Contrary to wild type cells or other previously mentioned knockouts the *vps24Δ* DOG sample hardly differs from the control. (Figure 12)

Disturbing PI3K by VPS34 gene deletion yielded death preventive results in the CSA and the PS localisation similarly shows little difference. The observed fuzzy accumulation close to the vacuole most likely is ER associated and appears in both samples. Lacking the distinct difference that the other DOG resistant knockouts vividly show, makes *vps34Δ* an odd case. However these findings support a core role of PIPs in the DOG response. (Figure 12)

5.9. Conclusion

In this study the adverse effects of DOG on yeast survival have been further unveiled. Activation of the Rim101 pathway appears to be a key event to trigger ESCRT-III formation [62, 64]. Until now the focus of examination was set on the alkaline pH response [55-65]. We focussed on the lipid transport, showing that prevention of cellular demise can be reached by impairment of Rim13 protease or ESCRT-III assembly.

Before deciding on the PS sensor, PE was checked for DOG interaction by addition of the lantibiotic cinnamycin, which enters the cell by binding to PE. The approach was discarded after initial screening. [82] (Supplemental Figure 2)

The findings by PS and PI4,5P_2 examination revealed PM involvement at crucial times during DOG stress. However the lack of congruency with the CSA results reveals that PM rearrangement is only one of the effects in the DOG stress response.

The combination of gene knockouts and microscopy including specific sensor molecules allowed for better understanding and additional ideas of involved

organelles and the route DOG takes after entering the cell, although other sensors should be included for completion and thorough understanding. By now, involvement of endocytic vesicles, EE, MVB and vacuole in the DOG entry route have been confirmed or strongly suggested. Further involvement of the RE and trans-Golgi network can be expected.

It appears that DOG is internalized, likely by clathrin-mediated endocytosis, shuttled via endocytic vesicles to the early endosome and further transported to the vacuole, where it is degraded. From the vacuole onwards DAG is either stored in TAG or broken down to monoacylglycerol and octanoic acid. Transport from the vacuole and LDs in case of previous storage to ER, Golgi or PM seems likely. Interaction of DAG with LDs and ER before reaching the vacuole is possible and probable.

An initial pulse-chase experiment to examine DAG movement after shifting the cells from DOG medium to minimal medium yielded inconclusive results, most likely due to suboptimal choice of incubation time. (Supplemental Figure 3)

5.10. Further experiments

Experiments of interest for expansion and completion of this work include further CSAs with cells carrying gene deletions involved in endocytosis and PL metabolism, colocalisation studies of the applied microscopic markers and localisation of other PIP-species.

Genes of interest for CSA of the PL biosynthesis pathway might be CHO1, the PS synthase; the PS decarboxylases PSD1 and PSD2, whereas PSD1 is located to the mitochondrion and PSD2 is located to Golgi and vacuole; CHO2, a PE methyltransferase and OPI3, a methylene-fatty-acyl-phospholipid synthase.

Furthermore, colocalisation studies with ER, LD and vacuole-markers are of interest for all sensors used in this study. Additionally endosomal colocalisation with DAG-sensor and PI4,5P_2 might elucidate some trafficking processes.

For some PIP-species like PI3P and PI4P sensor molecules already have been published. PI3P is specifically bound by the FYVE-domain of human early endosome antigen (EEA1) protein. [67] PI4P can be detected by the PH domain of OSH2 of *S. cerevisiae*, although binding of OSH2 to PI4,5P_2 in a reduced manner has been reported. [83]

In conclusion, the lipotoxicity pathway in yeast involves many organelles, each of which need to be considered when doing further investigation on the topic.

6. Supplemental Data

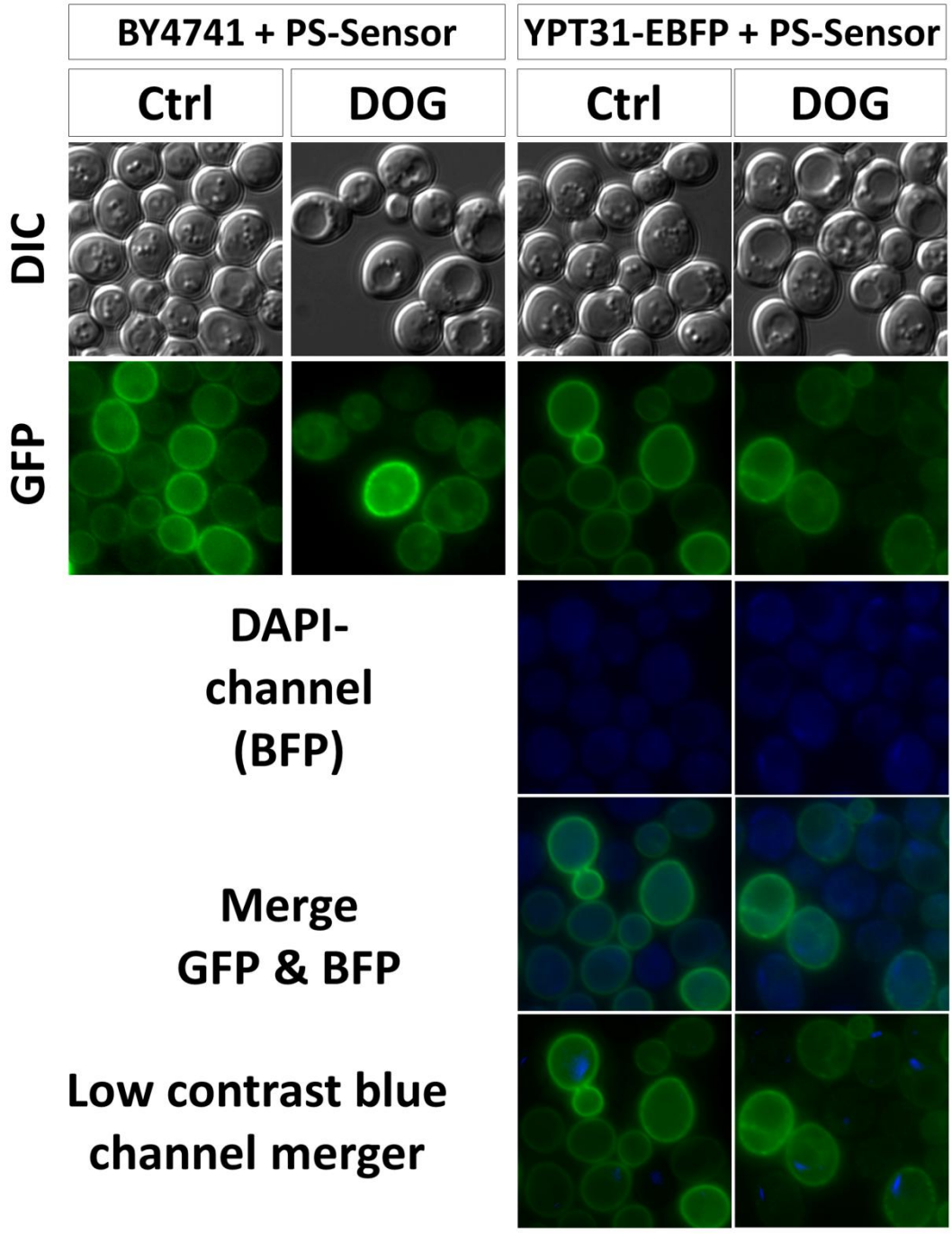

Supplemental Figure 1: Colocalisation of PS and RE. Images of *S. cerevisiae* wild type and YPT31-EBFP, each carrying the PS sensor plasmid under control conditions (CTRL, left) and DOG induced stress condition (right). Applied filters are DIC and GFP for both strains, DAPI for YPT31-EBFP to capture blue spectrum. Due to the nature of the DAPI filter its intensity had to be reduced digitally to match the GFP band pass filter.

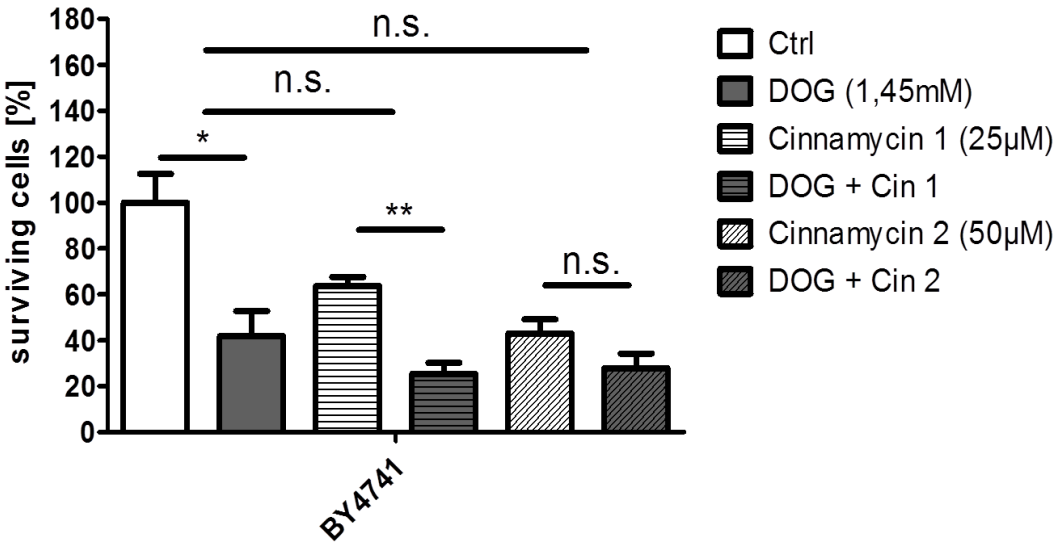

Supplemental Figure 2: CSA of wild type cells treated with DOG and/or cinnamycin. Y-scale depicts surviving cells in percent. 100% is set to wild type control. White bars represent control samples, grey bars represent lipid stress samples, dashed bars represent cinnamycin addition, dashed grey bars represent addition of DOG and cinnamycin. Asterisks indicate statistical significance tested by two-way-ANOVA. ($p < 0.05$ *, $p < 0.01$ **, $p < 0.001$ ***) Error bars represent standard error mean.

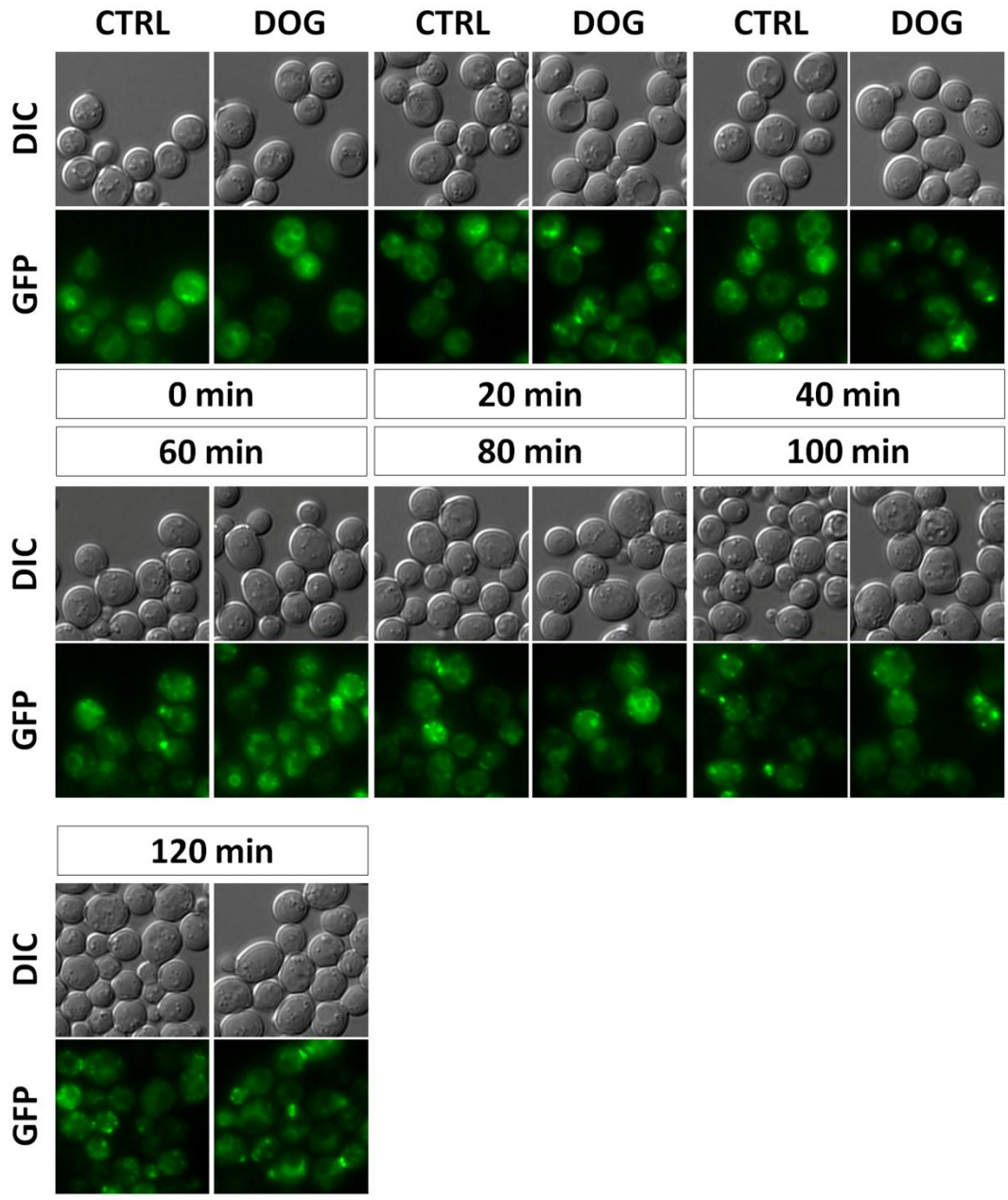

Supplemental Figure 3: DOG PulseChase experiment. Images of *S.cerevisiae* wild type cells carrying the DAG sensor plasmid und control conditions (CTRL, left) and DOG induced stress condition (right). Applied filters: DIC and GFP.

7. References

1. Fröhlich, K. U. & Madeo, F. Apoptosis in yeast--a monocellular organism exhibits altruistic behaviour. *FEBS Lett.* **473,** 6–9 (2000).
2. Büttner, S. *et al.* Endonuclease G Regulates Budding Yeast Life and Death. *Molecular Cell* **25,** 233–246 (2007).
3. Fröhlich, K. U. & Madeo, F. Apoptosis in yeast: a new model for aging research. *Exp. Gerontol*. **37**, 27–31 (2001).
4. Carmona-Gutierrez, D. et al. Apoptosis in yeast: triggers, pathways, subroutines. *Cell Death Differ.* **17**, 763–773 (2010).
5. Unger, R. H., Clark, G. O., Scherer, P. E. & Orci, L. Lipid homeostasis, lipotoxicity and the metabolic syndrome. *Biochim. Biophys. Acta* **1801**, 209–214 (2010).
6. Mager, W. H. & Winderickx, J. Yeast as a model for medical and medicinal research. *Trends Pharmacol. Sci.* **26**, 265–273 (2005).
7. Fröhlich, K.-U., Fussi, H. & Ruckenstuhl, C. Yeast apoptosis--from genes to pathways. *Semin. Cancer Biol.* **17**, 112–121 (2007).
8. Yeung, T. *et.al*. Membrane phosphatidylserine regulates surface charge and protein localisation. Science **319**, 210-212 (2008).
9. Tehlivets, O. *et. al*. Fatty acid synthesis and elongation in yeast. *Biochim. Biophys. Acta* **1771**, 255-270 (2007).
10. Kohlwein, S.D. Obese and anorexic yeasts: Experimental models to understand the metabolic syndrome and lipotoxicity. *Biochim. Biophys. Acta* **1801**, 222-229 (2010)
11. Deichmann, W.B. et.al. What is there that is not poison? A study of the Third Defense by Paracelsus. *Arch Toxicol*. **58**, 207-213 (1986).
12. Carmona-Gutierrez, D. et al. Ceramide triggers metacaspase-independent mitochondrial cell death in yeast. *Cell Cycle Georget. Tex* **10**, 3973–3978 (2011).
13. Rockenfeller, P. et al. Fatty acids trigger mitochondrion-dependent necrosis. *Cell Cycle Georget. Tex* **9**, 2836–2842 (2010).

14. Listenberger, L. L., Ory, D. S. & Schaffer, J. E. Palmitate-induced Apoptosis Can Occur through a Ceramide-independent Pathway. *J. Biol. Chem.* **276,** 14890–14895 (2001).
15. Brookheart, R. T., Michel, C. I. & Schaffer, J. E. As a Matter of Fat. *Cell Metab*. **10**, 9–12 (2009).
16. Listenberger, L. L. *et al*. Triglyceride accumulation protects against fatty acid-induced lipotoxicity. *Proc. Natl. Acad. Sci. U. S. A.* **100**, 3077–3082 (2003).
17. Kohlwein, S.D. Triacylglycerol homeostasis: insights from yeast. *Jour. Of. Biol. Chem.* **285**, 15663-15667 (2010)
18. Paltauf, F., *et al*. Regulation and compartmentalization of lipid synthesis in yeast. *Molecular and Cellular Biology of the Yeast Saccharomyces: Gene Expression.* 415-500 (1992)
19. Kennedy, E. P. & Weiss, S. B. The Function of Cytidine Coenzymes in the Biosynthesis of Phospholipides. *J. Biol. Chem.* **222,** 193–214 (1956).
20. Leventis, P. A. & Grinstein, S. The Distribution and Function of Phosphatidylserine in Cellular Membranes. *Annual Review of Biophysics* **39,** 407–427 (2010).
21. Fairn, G. D., Hermansson, M., Somerharju, P. & Grinstein, S. Phosphatidylserine is polarized and required for proper Cdc42 localization and for development of cell polarity. *Nat Cell Biol* **13,** 1424–1430 (2011).
22. Strahl, T., Thorner, J. Synthesis and function of membrane phosphoinositides in budding yeast, Saccharomyces cerevisiae. *Biochim Biophys Acta* **1771**, 353-404 (2007).
23. De Camilli, P., Emr, S.D., McPherson, P.S., Novick, P. Phosphoinositides as regulators in membrane traffic. *Science* **271**, 1533-1539 (1996).
24. York, J.D. Regulation of nuclear processes by inositol polyphosphates. *Biochim Biophys Acta* **1761**, 552-559 (2006).
25. Bennett, M., Onnebo, S.M., Azevedo, C., Saiardi, A. Inositol pyrophosphates: metabolism and signaling. *Cell Mol Life Sci* **63**, 552-564 (2006).
26. Bhandari, R., Chakraborty, A., Snyder, S.H. Inositol pyrophosphate pyrotechnics. *Cell Metab* **5**, 321-323 (2007).

27. Lester, R. L. & Steiner, M. R. The occurrence of diphosphoinositide and triphosphoinositide in Saccharomyces cerevisiae. *J. Biol. Chem.* **243,** 4889–4893 (1968).
28. Auger, K. R., Carpenter, C. L., Cantley, L. C. & Varticovski, L. Phosphatidylinositol 3-kinase and its novel product, phosphatidylinositol 3-phosphate, are present in Saccharomyces cerevisiae. *J. Biol. Chem.* **264,** 20181–20184 (1989).
29. Dove, S. K. *et al.* Osmotic stress activates phosphatidylinositol-3,5-bisphosphate synthesis. *Nature* **390,** 187–192 (1997).
30. Zolov, S. N. *et al.* In vivo, Pikfyve generates PI(3,5)P2, which serves as both a signaling lipid and the major precursor for PI5P. *Proc Natl Acad Sci U S A* **109,** 17472–17477 (2012).
31. Nunès JA, Guittard G. An Emerging Role for PI5P in T Cell Biology. *Frontiers in Immunology*. 2013;4:80. doi:10.3389/fimmu.2013.00080.
32. Mendonsa, R. & Engebrecht, J. Phosphatidylinositol-4,5-Bisphosphate and Phospholipase D-Generated Phosphatidic Acid Specify SNARE-Mediated Vesicle Fusion for Prospore Membrane Formation. *Eukaryotic Cell* **8,** 1094–1105 (2009).
33. Majerus, P. W. & York, J. D. Phosphoinositide phosphatases and disease. *J. Lipid Res.* **50,** S249–S254 (2009).
34. Petschnigg, J. et al. Good fat, essential cellular requirements for triacylglycerol synthesis to maintain membrane homeostasis in yeast. *J. Biol. Chem.* **284**, 30981–30993 (2009).
35. Coleman, R. A. & Lee, D. P. Enzymes of triacylglycerol synthesis and their regulation. *Prog. Lipid Res.* **43**, 134–176 (2004).
36. Klug, L. & Daum, G. Yeast lipid metabolism at a glance. *FEMS Yeast Res.* **14**, 369–388 (2014).
37. Black, P. N. & DiRusso, C. C. Yeast acyl-CoA synthetases at the crossroads of fatty acid metabolism and regulation. *Biochim. Biophys. Acta BBA - Mol. Cell Biol. Lipids* **1771**, 286–298 (2007).

38. Henry, S. A., Kohlwein, S. D. & Carman, G. M. Metabolism and Regulation of Glycerolipids in the Yeast Saccharomyces cerevisiae. *Genetics* **190**, 317–349 (2012).
39. Sorger, D. & Daum, G. Triacylglycerol biosynthesis in yeast. *Appl. Microbiol. Biotechnol.* **61**, 289–299 (2003).
40. Czabany, T., Athenstaedt, K. & Daum, G. Synthesis, storage and degradation of neutral lipids in yeast. *Biochim. Biophys. Acta BBA - Mol. Cell Biol. Lipids* **1771**, 299–309 (2007).
41. Carrasco, S. & Mérida, I. Diacylglycerol, when simplicity becomes complex. *Trends Biochem. Sci.* **32**, 27–36 (2007).
42. Ligr, M. et.al. Mammalian Bax triggers apoptotic changes in yeast. *FEBS Lett.* **438**, 61-65 (1998).
43. Galluzzi, L. et al. Molecular definitions of cell death subroutines: recommendations of the Nomenclature Committee on Cell Death 2012. *Cell Death Differ.* **19**, 107–120 (2012).
44. Golstein, P. & Kroemer, G. Cell death by necrosis: towards a molecular definition. *Trends Biochem. Sci.* **32**, 37–43 (2007).
45. Eisenberg, T., Carmona-Gutierrez, D., Büttner, S., Tavernarakis, N. & Madeo, F. Necrosis in yeast. *Apoptosis Int. J. Program. Cell Death* **15**, 257–268 (2010).
46. Walker, N. I., Harmon, B. V., Gobé, G. C. & Kerr, J. F. Patterns of cell death. *Methods Achiev. Exp. Pathol.* **13**, 18–54 (1988).
47. Vandenabeele, P., Galluzzi, L., Berghe, T. V. & Kroemer, G. Molecular mechanisms of necroptosis: an ordered cellular explosion. *Nature Reviews Molecular Cell Biology* **11,** 700–714 (2010).
48. Galluzzi, L. & Kroemer, G. Necroptosis: a specialized pathway of programmed necrosis. *Cell* **135**, 1161–1163 (2008).
49. Dudgeon, D. D., Zhang, N., Ositelu, O. O., Kim, H. & Cunningham, K. W. Nonapoptotic Death of Saccharomyces cerevisiae Cells That Is Stimulated by Hsp90 and Inhibited by Calcineurin and Cmk2 in Response to Endoplasmic Reticulum Stresses. *Eukaryot. Cell* **7**, 2037–2051 (2008).

50. Liang, Q. & Zhou, B. Copper and Manganese Induce Yeast Apoptosis via Different Pathways. *Mol Biol Cell* **18,** 4741–4749 (2007).
51. Madeo, F. *et al.* A Caspase-Related Protease Regulates Apoptosis in Yeast. *Molecular Cell* **9,** 911–917 (2002).
52. Wissing, S. *et al.* An AIF orthologue regulates apoptosis in yeast. *J Cell Biol* **166,** 969–974 (2004).
53. Chen, H., Workman, J. J., Tenga, A. & Laribee, R. N. Target of rapamycin signaling regulates high mobility group protein association to chromatin, which functions to suppress necrotic cell death. *Epigenetics Chromatin* **6,** 29 (2013).
54. Futai, E. *et al.* The protease activity of a calpain-like cysteine protease in Saccharomyces cerevisiae is required for alkaline adaptation and sporulation. *Mol. Gen. Genet.* **260,** 559–568 (1999).
55. Castrejon, F., Gomez, A., Sanz, M., Duran, A. & Roncero, C. The RIM101 Pathway Contributes to Yeast Cell Wall Assembly and Its Function Becomes Essential in the Absence of Mitogen-Activated Protein Kinase Slt2p. *Eukaryot Cell* **5,** 507–517 (2006).
56. Ikeda, M., Kihara, A., Denpoh, A. & Igarashi, Y. The Rim101 pathway is involved in Rsb1 expression induced by altered lipid asymmetry. *Mol. Biol. Cell* **19,** 1922–1931 (2008).
57. Obara, K. & Kihara, A. Signaling events of the Rim101 pathway occur at the plasma membrane in a ubiquitination-dependent manner. *Mol. Cell. Biol.* **34,** 3525–3534 (2014).
58. Mitchell, A. P. A VAST staging area for regulatory proteins. *Proc. Natl. Acad. Sci. U.S.A.* **105,** 7111–7112 (2008).
59. Mousley, C. J. *et al.* A sterol-binding protein integrates endosomal lipid metabolism with TOR signaling and nitrogen sensing. *Cell* **148,** 702–715 (2012).
60. Lamb, T. M. & Mitchell, A. P. The transcription factor Rim101p governs ion tolerance and cell differentiation by direct repression of the regulatory genes NRG1 and SMP1 in Saccharomyces cerevisiae. *Mol. Cell. Biol.* **23,** 677–686 (2003).

61. Obara, K., Yamamoto, H. & Kihara, A. Membrane Protein Rim21 Plays a Central Role in Sensing Ambient pH in Saccharomyces cerevisiae. *J Biol Chem* **287,** 38473–38481 (2012).
62. Calcagno-Pizarelli, A. M. *et al.* Rescue of Aspergillus nidulans severely debilitating null mutations in ESCRT-0, I, II and III genes by inactivation of a salt-tolerance pathway allows examination of ESCRT gene roles in pH signalling. *J. Cell. Sci.* **124,** 4064–4076 (2011).
63. Gomez-Raja, J. & Davis, D. A. The β-arrestin-like protein Rim8 is hyperphosphorylated and complexes with Rim21 and Rim101 to promote adaptation to neutral-alkaline pH. *Eukaryotic Cell* **11,** 683–693 (2012).
64. Hayashi, M., Fukuzawa, T., Sorimachi, H. & Maeda, T. Constitutive activation of the pH-responsive Rim101 pathway in yeast mutants defective in late steps of the MVB/ESCRT pathway. *Mol. Cell. Biol.* **25,** 9478–9490 (2005).
65. Galindo, A., Calcagno-Pizarelli, A. M., Arst, H. N. & Peñalva, M. Á. An ordered pathway for the assembly of fungal ESCRT-containing ambient pH signalling complexes at the plasma membrane. *J. Cell. Sci.* **125,** 1784–1795 (2012).
66. Goode BL, Eskin JA, Wendland B. Actin and Endocytosis in Budding Yeast. *Genetics*. **199**, 315–358 (2005).
67. Burd, G., & Emr, S.D. Phosphatidylinositol(3)-Phosphate Signaling Mediated by Specific Binding to RING FYVE Domains. *Molecular Cell.* **2**, 157-162 (1998).
68. Li, G. et.al. Evidence for phosphatidyl-inositol 3-kinase as a regulator of endocytosis via activation of Rab5. *Proc. Natl. Acad. Sci. USA* **92**, 10207–10211 (1995).
69. Bowers, K., & Stevens, T.H. Protein transport from the late Golgi to the vacuole in the yeast *Saccharomyces cerevisiae*. *Biochim. Biophys. Acta.* **1744**, 438-454 (2005).
70. Baldehaar, H.J. et.al. The Rab GTPase Ypt7 is linked to retromer-mediated receptor recycling and fusion at the yeast late endosome. *Journal of Cell Science.* **123**, 4085-4094 (2010)

71. van IJzendoorn, S.C.D. Recycling endosomes. *Journal of Cell Science*. **119**, 1679–81 (2006).
72. Benli, M. et.al. Two GTPase isoforms, Ypt31p and Ypt32p, are essential for Golgi function in yeast. *EMBO*. **15**, 6460-6475 (1996)
73. Munn, A. L. & Riezman, H. Endocytosis is required for the growth of vacuolar H(+)-ATPase-defective yeast: identification of six new END genes. *J. Cell Biol.* **127,** 373–386 (1994).
74. Knop, M. *et al.* Epitope tagging of yeast genes using a PCR-based strategy: more tags and improved practical routines. *Yeast* **15,** 963–972 (1999).
75. Stefan, C. J., Audhya, A. & Emr, S. D. The Yeast Synaptojanin-like Proteins Control the Cellular Distribution of Phosphatidylinositol (4,5)-Bisphosphate. *Mol. Biol. Cell* **13,** 542–557 (2002).
76. Kim, Y. J., Guzman-Hernandez, M. L. & Balla, T. A Highly Dynamic ER-Derived Phosphatidylinositol-Synthesizing Organelle Supplies Phosphoinositides to Cellular Membranes. *Developmental Cell* **21,** 813–824 (2011).
77. Linkert, M. *et al.* Metadata matters: access to image data in the real world. *J Cell Biol* **189,** 777–782 (2010).
78. Schindelin, J. *et al.* Fiji: an open-source platform for biological-image analysis. *Nat Meth* **9,** 676–682 (2012).
79. Schneider, C. A., Rasband, W. S. & Eliceiri, K. W. NIH Image to ImageJ: 25 years of image analysis. *Nat Meth* **9,** 671–675 (2012).
80. Unk, I. & Dabara, A. Synchronization of Saccharomyces cerevisiae Cells in G1 Phase of the Cell Cycle. *bio-protocol* **4,** (2014).
81. Tkach, J. M. *et al.* Dissecting DNA damage response pathways by analyzing protein localization and abundance changes during DNA replication stress. *Nat Cell Biol* **14,** 966–976 (2012).
82. Makino, A. *et al.* Cinnamycin (Ro 09-0198) Promotes Cell Binding and Toxicity by Inducing Transbilayer Lipid Movement. *J. Biol. Chem.* **278,** 3204–3209 (2003).

83. Hammond, G. R. V. & Balla, T. Polyphosphoinositide binding domains: Key to inositol lipid biology., Polyphosphoinositide binding domains: key to inositol lipid biology. *Biochim Biophys Acta* **1851,** 746–758 (2015).
84. Boysen, J. H. & Mitchell, A. P. Control of Bro1-domain protein Rim20 localization by external pH, ESCRT machinery, and the Saccharomyces cerevisiae Rim101 pathway. *Mol. Biol. Cell* **17,** 1344–1353 (2006).
85. Fratti, R. A., Collins, K. M., Hickey, C. M. & Wickner, W. Stringent 3Q·1R Composition of the SNARE 0-Layer Can Be Bypassed for Fusion by Compensatory SNARE Mutation or by Lipid Bilayer Modification. *J. Biol. Chem.* **282,** 14861–14867 (2007).